

PREPARED FOR SUBMISSION TO JCAP

Search for anomalous features in gamma-ray blazar spectra corrected for the absorption on the extragalactic background light

Alexander Korochkin,^{a,b} Grigory Rubtsov^a and Sergey Troitsky^a

^aInstitute for Nuclear Research of the Russian Academy of Sciences,
60th October Anniversary Prospect 7a, Moscow 117312, Russia

^bAPC, Université Paris Diderot, Bâtiment Condorcet, Case 7020,
75205 Paris Cedex 13, France

E-mail: st@ms2.inr.ac.ru

Abstract. We consider the ensemble of very-high-energy gamma-ray sources observed at distances and energies where a significant absorption of gamma rays is expected due to pair production on the extragalactic background light (EBL). Previous studies indicated that spectra of these sources, upon correction for the absorption, exhibit unusual spectral hardenings which happen precisely at the energies where the correction becomes significant. Here, we address this subject with the most recent clean sample of distant gamma-ray blazars, making use of published results of imaging atmospheric Cerenkov telescopes and of the Fermi-LAT Pass 8 data, supplemented by the newest absorption models and individual measurements of sources' redshifts. We perform a search for spectral breaks at energies corresponding to unit optical depth with respect to the absorption on EBL. These energies are different for distant and nearby objects, and consequently, such features may not be related to intrinsic properties of the sources. While in some spectra such breaks are not seen, hardenings at distance-dependent energies are present in many of them, though the overall statistical significance of the effect is lower than reported in previous studies. The dependence of the break strength on the redshift found earlier is not confirmed in the new analysis.

Contents

1	Introduction	1
2	The data	5
2.1	Selection criteria	5
2.2	IACT subsample	7
2.3	Fermi-LAT subsample	8
2.4	The sample	9
3	Data analysis and results	9
4	Discussion	12
4.1	Systematic uncertainties	13
4.1.1	Absorption models	13
4.1.2	The Malmquist bias	14
4.1.3	Source classes	16
4.1.4	Tail of the falling spectrum	16
4.1.5	Redshifts	18
4.2	Comparison to previous studies	19
4.2.1	Rubtsov and Troitsky (2014) [19]	19
4.2.2	Horns and Meyer (2012) [18]	19
4.2.3	Fermi-LAT collaboration (2012) [13]	20
4.2.4	Biteau and Williams (2015) [11]	21
4.2.5	Galanti et al. (2015) [93]	23
4.2.6	Studies of high-energy versus very-high-energy spectral indices	23
5	Conclusions	24
A	Observed and best-fit intrinsic spectra of blazars in the main sample.	25

1 Introduction

It is well known since 1960s [1] that energetic gamma rays produce electron-positron pairs on the extragalactic background light (EBL). Because of this process, gamma-ray flux from distant sources is attenuated severely and the propagation distance is limited. Very-high-energy (VHE) gamma rays (energy $E \gtrsim 100$ GeV) scatter most efficiently on the infrared and

visible background photons, and information on the intergalactic absorption may be deduced from VHE observations of emitters located at cosmologically large distances.

There exists some long-standing controversy in the determination of the EBL intensity, with direct measurements indicating consistently higher EBL than indirect constraints do. Direct observations are very difficult to carry out because of strong foreground contamination by the Zodiacal light and by the Galactic foreground. Nevertheless, numerous attempts gave coherent, though quite uncertain, results [2–6]. At the same time, there are two groups of methods that set lower and upper limits on the EBL. The first group is based on the deep field observations of the Universe. This approach uses the method of galactic counts and results in lower limits on the EBL intensity, given just by the sum of contributions from guaranteed light sources [7–9]. On the other hand, upper constraints come from gamma-ray observations of blazars [10–13]. As the VHE part of the blazars spectra is highly absorbed by the EBL, the requirement that the intrinsic spectrum is not too hard, or is a smooth extrapolation from lower energies, provides constraints on the attenuation and thus on the EBL. These gamma-ray upper limits assume standard absorption on the EBL and therefore cannot be used in a work testing possible deviations from this standard picture. Finally, numerical simulations include more theoretical input from the star formation rate history but point to a similar range of intensities as the galaxy-count methods. The situation remains unsettled: two independent observations, published in 2017 and using different sophisticated techniques to get rid of the foreground systematics [6, 14], point consistently to the EBL intensities considerably higher than the most recent theoretical models. For the purposes of the present study, we need a conservative (low-absorption) model and use that of Korochkin and Rubtsov (2018) [15] as the most recent available benchmark for the low-EBL theoretical models. Variations of the absorption model will be discussed in the context of systematic uncertainties of our results.

Distant blazars are observed in energetic gamma rays from the early days of the VHE astronomy. It has been pointed out long ago that some of them are seen from distances for which the optical depth with respect to the pair production on EBL is significant. This apparent tension with expectations was dubbed “the infrared/TeV crisis” [16]. However, subsequent improvements in EBL models demonstrated that the tension is not that strong. While apparent hardening of the intrinsic spectrum (corrected for the pair-production attenuation, that is “deabsorbed”), seen in several individual sources, might be related to physical conditions in particular objects, a successful model for these hardenings is missing [17].

The situation has been changed when the number of sources observed at large optical depths became sufficient for studies of their ensembles. The study of a sample of 7 sources observed by imaging atmospheric Cerenkov telescopes (IACTs) at optical depths $\tau \gtrsim 2$ by

Horns and Meyer [18] suggested that the energy at which these hardenings happen is correlated with the distance to the source in such a way that the spectra become harder only when the correction for the pair-production absorption is significant. This correlation can hardly be caused by any physical reason and suggests that the optical depth is estimated incorrectly. The statistical significance of this “pair-production anomaly” was estimated at the $\sim 4\sigma$ level ¹².

The largest sample of sources detected at large optical depths ($\tau \gtrsim 1$, 15 objects observed by IACTs and 5 objects observed by Fermi Large Area Telescope, LAT) has been considered [19] in 2014. There, we first confirmed the existence of significant hardenings in deabsorbed spectra of a number of objects at the energies where the correction for pair production becomes important. We then considered the full sample of objects, including those with and without statistically significant hardenings, and fit their deabsorbed spectra with the broken power-law function, assuming the break at the energy E_0 , at which the pair-production optical depth $\tau(E_0) = 1$ (these energies are different for sources at different redshifts). We found that the break strength, that is the difference between power-law indices below and above E_0 , grows with the source redshift z . Assuming the growth linear in $\log z$, the statistical significance of this distance dependence, again suggesting an unphysical origin of the hardenings and hence an incorrect account of the absorption, was found to be $\sim 12\sigma$.

All these results are of great importance not only for the gamma-ray astronomy, but also for other fields of physics and astrophysics. As it will be discussed below, overestimation of the absorption can hardly be understood without invoking new physical or astrophysical phenomena, and its most promising explanation requires the existence of new light particles beyond those described by the Standard Model of particle physics.

Since 2014, several important improvements changed the field. Firstly, many new observations of distant VHE blazars have been performed by IACTs. Secondly, the Fermi-LAT team not only accumulated additional years of statistics, very important for faint distant VHE sources, but also issued the new “Pass 8” reconstruction [20] improving the data processing. Another related novelty is the 3FHL catalog [21] of hard-spectrum sources making pre-selection of the sample easier and more uniform than before. Thirdly, from the EBL side, new and improved conservative theoretical models have become available [15, 22, 23], but at the same time new sophisticated observational studies strengthened the tension in the

¹Hereafter, we quote statistical significances in terms of standard deviations, σ , as it is customary in the high-energy physics. One should always understand the following meaning of these estimates: the probability that the observed, or stronger, effect appears as a random fluctuation is the same as it would happen for a normally distributed random quantity deviating from the mean by this number of standard deviations. The underlying probability distribution is never Gaussian in the analyses we discuss.

²See also the discussion of tests [11] of this result in Sec. 4.2.4.

determination of the background radiation intensity [6, 14]. Finally, for a number of objects, new information on their redshifts became available. The main purpose of this work is to revisit the claims of Refs. [18, 19] with an extended high-quality sample of sources, taking into account all the listed improvements and making use of a more conservative analysis method. We also present some tests demonstrating independence of our results from potential biases and their stability with respect to systematic uncertainties. The result of the present study favours the presence of spectral features precisely at the energies for which the correction becomes important, though with a significance of only $\sim 2\sigma$. However, we do not confirm the distance dependence of the break strengths.

The rest of the paper is organized as follows. In Sec. 2, we discuss gamma-ray data used in our study. Section 2.1 summarizes general criteria for the sample construction. Section 2.2 detalizes how they are implemented for the objects observed by IACTs, while Sec. 2.3 discusses the construction of the Fermi-LAT subsample. We list the resulting sample of 31 sources and discuss its general properties in Sec. 2.4.

Section 3 describes the data analysis procedure and presents the main results of the paper. We describe how the correction to the pair-production opacity is implemented and perform a combined analysis of the full sample of 31 sources. We fit all the spectra with absorbed broken power laws, assuming that the break energy E_b is a free parameter, and demonstrate that the fits suggest $E_b \approx E_0(z)$. Then, we repeat the fits with fixed $E_b = E_0(z)$ and demonstrate that indeed spectral features at the distance-dependent energies are slightly favoured. This result is discussed in detail in Sec. 4. There, we first turn, in Sec. 4.1, to potential biases and systematic uncertainties which might affect our result. In Sec. 4.1.1, we discuss variations in the absorption model: besides the most recent model we use throughout the paper, Korochkin and Rubtsov (2018) [15], we repeat our analysis with three other EBL models, namely: Gilmore et al. (2012) fixed [24], which was used in our 2014 paper; Franceschini and Rodighiero (2017) [23]; and a toy upper-limit model artificially normalized to the most recent direct observational data [6, 14] on the background-light intensity. Next, in Sec. 4.1.2, we discuss a possible bias related to the fact that only brightest sources are seen at large distances, the Malmquist bias. We extend our sample to include numerous sources not detected in the highest-energy spectral bins, but satisfying at the same time all other selection criteria. We use flux upper limits for the undetected sources and demonstrate that they are consistent with the results of Sec. 3. In Sec. 4.1.3, we address another potential bias related to the fact that, generally, blazars detected at higher redshifts are mostly flat-spectrum radio quasars (FSRQs) while those at lower redshifts are mostly BL Lac type objects (BLLs). FSRQs might have intrinsic features in the spectrum which mimic the distance dependence just because all observed FSRQs are distant. We demonstrate that the problematic

spectral features do not depend on the synchrotron peak frequency often used to distinguish between different classes of blazars. In Sec. 4.1.4, we discuss the effect of uncertainties in the energy determination, which may have important consequences for the estimation of the spectral shape at the highest energies for steeply falling spectra. We perform various tests and conclude that this effect is unlikely to affect our results. Finally, in Sec. 4.1.5 we attempt to estimate a potential impact of possible wrong determination of distances to the sources. Since 2014, new redshift data removed 4 of 20 sources from the original sample of Ref. [19]. We randomly remove 1, 2 or 3 sources from our new sample of 31 objects and demonstrate that, in most cases, this does not change significantly our results, therefore suggesting that (a reasonable number of) erroneous redshifts can hardly cause the effect we observe. Therefore, we conclude that none of the biases or uncertainties we are aware of may affect the principal result of the paper, and continue in Sec. 4.2 with a brief account of novelties and differences of this result in comparison with previous studies.

While the outline of our study and a summary of results are given in this Introduction, we present a brief account of our conclusions and discuss possible approaches to the interpretation of our results in Sec. 5. Appendix A presents observed and best-fit deabsorbed spectra of 31 blazars entering our main sample.

2 The data

2.1 Selection criteria

The purpose of the present study implies the use of high-quality gamma-ray spectra of sources located at large, confidently known distances. The obvious candidates are blazars with firmly measured redshifts. For various redshifts z , the absorption due to e^+e^- pair production becomes important at different energies of photons: for more distant sources, pair production affects the spectra at lower energies³. The benchmark energy, at which the absorption becomes important, corresponds to the optical depth $\tau = 1$ and is denoted as E_0 hereafter,

$$\tau(E_0, z) = 1,$$

which determines $E_0(z)$ for a given absorption model, see Fig. 1.

To study the behaviour of a spectrum in the region of strong absorption, one needs observations at $E \gtrsim E_0$; therefore, the use of different instruments is required for objects located at different redshifts: for large z , E_0 is typically dozens of GeV, and the relevant instrument is Fermi LAT, while for less distant objects, E_0 is of order of several hundred GeV, and the data of IACTs should be used. Though the data are published in quite different

³This is true for energies below ~ 100 TeV which we discuss here.

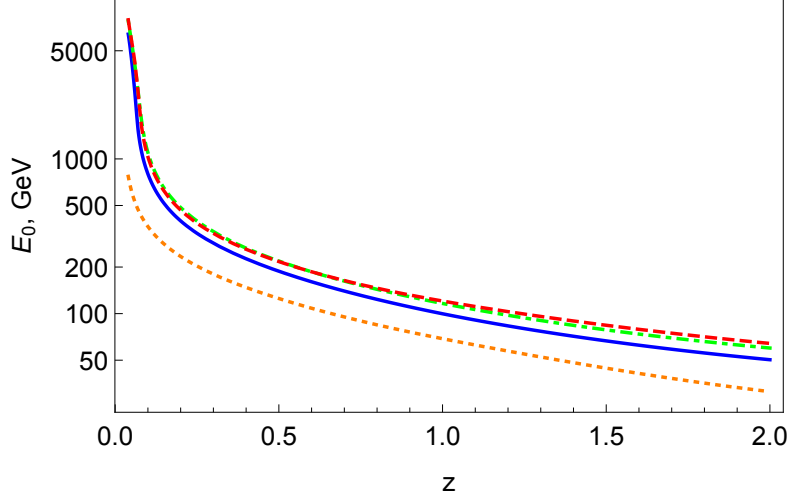


Figure 1. The energy E_0 corresponding to the pair-production optical depth $\tau = 1$ as a function of the redshift z for different absorption models: Korochnik and Rubtsov (2018) [15] (full line); Franceschini et al. (2017) [23] (dashed line); Gilmore et al. (2012) fixed [24] (dash-dotted line); and the toy high-absorption model discussed in Sec. 4.1.1 (dotted line).

ways, it is essential to treat them on equal footing. Here we discuss our general requirements governing selection of the objects, which will be implemented in the next two subsections for the Fermi-LAT and IACT data.

Redshift criteria. Incorrectly determined or uncertain redshifts may hurt any of blazar studies. This happens quite often, especially for BLLs whose spectra do not possess strong emission lines. We require a firm spectroscopic redshift for the objects included into our sample. More specifically, we start from a preselected sample of gamma-ray blazars and check, for every object, the relevant redshift information and references in the NASA/IPAC Extragalactic Database (NED)⁴. The redshifts are accepted if they satisfy (R1) and one of (R2A), (R2B), (R2C) criteria:

(R1) the redshift is spectroscopic (not photometric) and is derived from *emission* lines⁵
AND

EITHER (R2A) the redshift is determined in a dedicated study (if several dedicated studies give different results, the latest one is used),

OR (R2B) the redshift quoted in NED is determined in 2dF Galaxy Redshift Survey [25] or 6dF Galaxy Survey [26],

⁴Available at <http://ned.ipac.caltech.edu>.

⁵Since the absorption-line redshift gives a lower limit to the actual one, inclusion of objects with emission lines in the spectra would be conservative in terms of the search of anomalies; however, we removed 4 such objects from the sample following the Reviewer’s comment.

OR (R2C) the redshift quoted in NED is determined in the Sloan Digital Sky Survey (SDSS), the result is unique and does not change from one release to another.

These criteria are based on the previous experience in the use of redshift data and are of course ad hoc ones. Their application removes many uncertain redshifts.

Spectral criteria. In our work, we use binned gamma-ray spectra, because only this information is publicly available for the objects observed by IACTs. We impose the following criteria for the spectra:

(S1) information for at least 5 energy bins is available;

(S2) the lowest energy E_{last} of the last spectral bin satisfies $E_{\text{last}} > E_0$ AND the lowest energy of the third from below spectral bin is below E_0 .

These criteria are aimed at the reconstruction of spectra at E both below and above E_0 with reasonable accuracy.

Several comments are in order. Firstly, (S2) depends on the assumed absorption model, and therefore the samples we use in Sec. 4.1.1, when studying the sensitivity of our results to the choice of this model, are slightly different one from another. Secondly, while we require a nonzero measurement in the last bin for our main study, we allow for an upper limit when studying potential effects of the Malmquist bias in Sec. 4.1.2.

2.2 IACT subsample

To construct the sample of blazars observed by IACTs, we start with the database consolidating results published by different observatories, the TeVCat online source catalog [27]⁶. The preselected sample includes objects classified as blazars there (classes “HBL”, “IBL”, “LBL”, “BL Lac (class uncertain)”, “FSRQ” and “blazar”), 72 objects in total as of 2019. Then, for each object in the sample, we checked the redshift selection rules (R1) and ((R2A) or (R2B) or (R2C)), using references from NED, and availability of gamma-ray spectra satisfying (S1), using references from TeVCat.

Some objects have been observed several times, often by multiple instruments. To avoid double counting of information, which may artificially increase or dilute observed effects, we use only one observation for each source. It is chosen on the basis of better statistics (larger effective exposure in $\text{cm}^2\cdot\text{s}$). Because of strong variability of many blazars, we never combine any two spectra from observations performed at different epochs to extend the energy coverage. We also never combine Fermi-LAT spectra with those obtained from IACT observations because of potential systematic differences between the instruments’ energy scales. These requirements represent a major refinement with respect to some of preceding studies.

⁶Available at <http://tevcat.uchicago.edu>.

The next step requires to fix the absorption model. We use the most recent EBL model [15] as our baseline low-absorption model; when variations of the model are considered (Sec. 4.1.1), this step is repeated. At this step, we calculate the value of E_0 for every source and check the condition (S2). We are left with 26 objects which, together with the sources observed by Fermi LAT, are listed in Table 1.

2.3 Fermi-LAT subsample

For blazars observed by Fermi LAT, our starting point is the 3rd Fermi-LAT Catalog of High-Energy Sources, 3FHL [21]⁷, presenting a list of sources detected confidently above 10 GeV. From the catalog, we select 1212 objects classified as blazars (classes “BLL”, “blI”, “FSRQ”, “fsrq”, “bcu”). Since the redshifts presented in the catalog may be doubtful or erroneous for distant sources, we check them manually to satisfy (R1) and ((R2A) or (R2B) or (R2C)) criteria, using references from NED, and apply a preselection constraint $z \geq 0.2$, which is a consequence of (S2) and the Fermi-LAT energy coverage: for less distant sources, $E_0 \gtrsim 500$ GeV, that is beyond the limit of reasonable sensitivity of Fermi LAT. This procedure results in a list of 309 blazars. For each of them, we use publicly available Fermi-LAT [28] data⁸ to construct binned spectra satisfying (S1) automatically with the help of standard routines from Fermi Science Tools 1.0.1. To this end, we use Fermi Pass 8 [20] Release 3 data (version 303). We use “SOURCE” class events with version 2 instrumental response functions “P8R3_SOURCE_V2”, recorded between August 4, 2008, and February 26, 2018 (Mission Elapsed Time interval 239557417 – 541338374). The background models used are “gll_iem_v06.fits” for the Galactic component and “iso_P8R3_SOURCE_V2.txt” for the isotropic one. The background model also includes other sources from 3FGL catalog within 5° angular distance from the given source. For most of the sources (305 of 309), the coordinates of the source are taken from the 3rd Fermi-LAT Source Catalog, 3FGL [29]. However, not all 3FHL sources have 3FGL counterparts, and for the remaining 4 sources, we used 3FHL coordinates.

Firstly, we have performed an independent fit with the standard `gtlike` routine with the power-law spectrum model “PowerLaw2” in each of 8 energy bins with the width of 0.3 dex, for $E \geq 2$ GeV. The lower energy limit of 2 GeV was chosen to cut the inverse-Compton peak energy range in order to improve broken power-law fits used in our subsequent analysis.

Despite the fact that the use of `gtlike` is the preferred method of constructing sources’ spectra, it demonstrates an unstable behavior when the estimated number of counts in the energy bin is lower than one. In particular, the fit may not converge or converge to zero flux with unphysical value of the flux upper limit. Moreover, even when the number of photons is less than three, the estimated confidence interval for the flux follows the simple symmetric

⁷Available at <http://fermi.gsfc.nasa.gov/ssc/data/access/lat/3FHL/> .

⁸Available at <https://heasarc.gsfc.nasa.gov/FTP/fermi/data/lat/weekly/photon/> .

Gaussian distribution but not the Poisson one, as it should. Clearly these features may affect further analysis and to avoid the peculiar behavior of the fit optimization procedure we have stepped one level back to use the Fermi Science Tools routines which provide an input for `gtlike`. Namely, the standard `gtsrcprob` routine assigned the weight to each photon which is the probability to originate from a given source within the given source model. The sum of the corresponding weights provides an estimate for the number of photons from the given source and from each of the background sources.

At the next step, we fix the absorption model and apply the criterion (S2) to the obtained spectra. For the Fermi-LAT subsample, the criterion is used as follows: the source is accepted if it has at least one photon in the bin above E_0 and the probability that this photon is associated with the source is more than 99% (according to the `gtsrcprob` output). Only 5 of 309 blazars satisfy (S2) and enter our final sample.

Finally, for the bins which contain less than three photons we have replaced the `gtlike` flux with one obtained from summing weights from `gtsrcprob`. Since the background photons are considered separately, this sum may be treated as the number of signal events with zero background. We round this number to an integer (0 or 1 in most cases) and estimate the Poisson-based 68% CL interval for the flux in these bins by division by the exposure calculated with the `gtexpcube` routine. We have checked that the above procedure results in the value which agrees within 10% with the output of `gtlike` in cases when the latter converges to a physical value.

2.4 The sample

The list of 31 objects selected in the way described above, Sec. 2.2, 2.3, is presented in Table 1. For IACT observations, references for binned spectra used in this work are given there. We also list classes of the blazars (BLL or FSRQ) as determined in the catalogs used to compile the samples, TeVCat and 3FHL. In addition⁹, we give also references to original spectroscopic measurements of redshifts.

Figure 2 represents the distribution of blazars in our main sample in redshift. One may note that, though BLLs dominate at short and moderate distances and FSRQs are in general farther away, both classes cover large ranges of redshifts. We will return to this subject in Sec. 4.1.3.

3 Data analysis and results

The key point of our study is the use of blazar spectra corrected for the pair production in a minimal-absorption model. Since, for IACT observations, only binned spectra are available,

⁹Following a request of the anonymous referee.

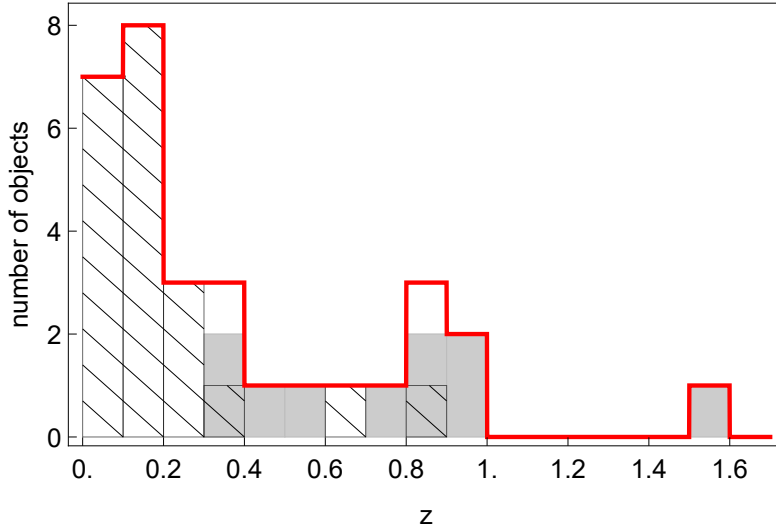


Figure 2. Distribution of 31 objects from the sample in redshift (full red histogram). Hatched and shaded histograms give separate distributions for BLLs and FSRQs, respectively.

we adopt our analysis procedure for this case even for Fermi LAT, in order to process all observations in a uniform way. In contrast with many previous studies, we do not use bin-by-bin deabsorption because it can introduce systematic biases in the highest-energy bins for the following reasons. The optical depth τ is a function of the incoming photon energy E and the source redshift z . It is important to note that the absorption is not uniform within the bin: photons of higher energy are absorbed stronger¹⁰. For the energies and distances at which the absorption is significant, this effect may affect strongly the result. It can be taken into account if the shape of the observed spectrum within the bin is known, as we have done in Ref. [19]; however, in practice, statistical uncertainties in the highest energy bins often make the determination of the shape uncertain. The uncertainty of the spectral shape within the bin translates into the error of deabsorbed flux. The latter effect is enhanced in bins, within which the absorption effect grows dramatically. It is shown that for wide energy bins of 0.3 dex used for the analysis of Fermi LAT sources, the uncertainty related to deabsorption contributes significantly to the flux error in energy bins above E_0 . Therefore the absorption of the model spectra instead of the deabsorption of the observed one is performed in our analysis.

Following the logic of previous studies, we start from the assumption about the intrinsic spectrum of a blazar, for which we use a broken power law. First, we make the break energy E_b a free parameter of the fit, so that it is adjusted independently for every source. We account for the absorption with the selected EBL model, integrate the obtained spectrum over the

¹⁰See footnote on page 5.

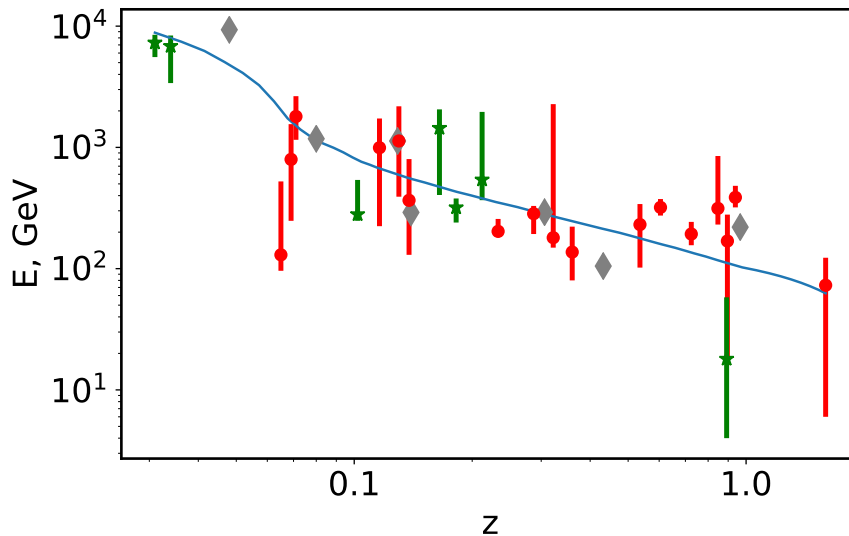


Figure 3. Positions of the break energies (red points: hardenings, green asterisks: softening), treated as free parameters in independent fits, compared to $E_0(z)$ (red line). Objects for which the broken power-law fit is not better than the power-law fit by $\Delta\chi^2 < 1$, that is for which best-fit break is consistent with zero, are shown as gray diamonds (since the error bars are determined by $\Delta\chi^2 = 1$ [85], they are infinite for these points).

energy bins and compare resulted bin-by-bin fluxes with the observed data points. In this way, we fit the data with the four parameters of the intrinsic spectrum, that is the overall normalization, the break position E_b , the spectral index at $E < E_b$ and $\Delta\Gamma$, the difference between spectral indices at $E > E_b$ and $E < E_b$. Technically, all our fits are performed with the method described in detail in Ref. [85]. Figure 3 compares the fitted break positions E_b with the value of $E_0(z)$; we see that they agree well to each other: averaged over the sample, $\log_{10}(E_b/E_0(z)) = -0.02 \pm 0.37$ (for 22 sources with positive breaks, i.e. spectral hardenings, we get 0.01 ± 0.36).

Then, we turn to similar fits with the break energy fixed at $E_b = E_0(z)$. Recall that this energy depends on the redshift of the source z , cf. Fig. 1, and therefore we assume breaks at different energies for different sources. Values of $\Delta\Gamma$ obtained in this way for individual sources are given in Appendix A and graphically presented in Fig. 4. One sees that while some spectra have $\Delta\Gamma$ consistent with zero, indications for $\Delta\Gamma > 0$ exist in many cases. For the entire sample, the assumption of $\Delta\Gamma = 0$ results in $\chi^2 = 44.0$ for 31 degrees of freedom, corresponding to the probability $P \simeq 0.06$ for the observed values of $\Delta\Gamma$ at $E_0(z)$ to occur as a result of a random fluctuation. Therefore, our results disagree with the hypothesis of the absence of breaks at $E_0(z)$ at 1.9 standard deviations (recall the footnote at p. 3 for our

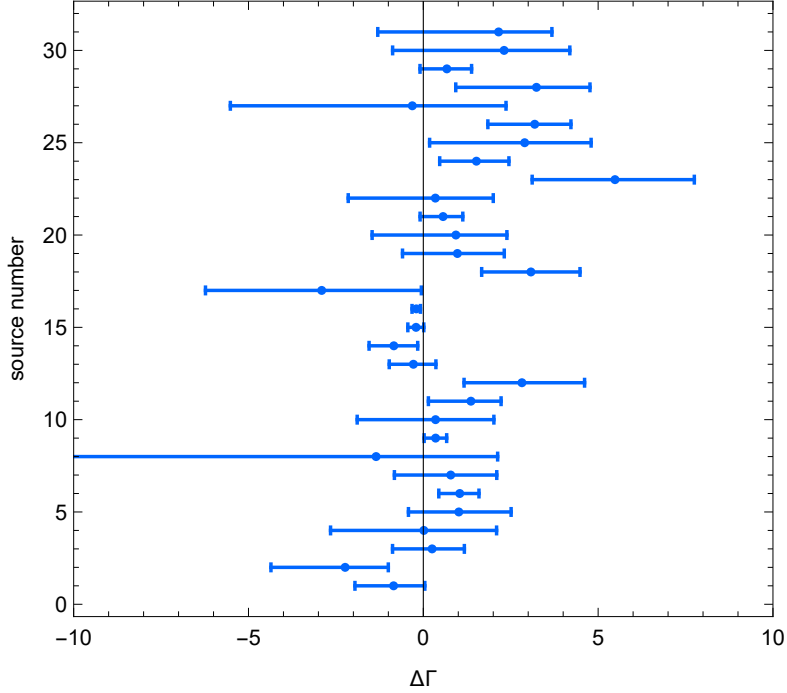


Figure 4. Breaks in deabsorbed blazar spectra at $E_b = E_0(z)$. See the text for details.

conventions)¹¹.

We can compare the assumption of breaks at $E_0(z)$ with that of breaks at some distance-independent energy, common to all sources. To this end, we perform fits of all spectral data by absorbed broken power laws, fixing the common break energy E_b for all objects in the sample, for various values of E_b . For every E_b , we determine the goodness of the fit, p , from the chi-squared distribution with the corresponding number of degrees of freedom (for 225 data points, 31 spectra fitted with 3 parameters each, the number of degrees of freedom is 132). The plot of $(1 - p)$ as a function of E_b is shown in Fig. 5 (the best possible fit would correspond to $(1 - p) = 0$, a very bad fit – to $(1 - p) \approx 1$), together with the same quantity calculated for fits with breaks at $E_0(z)$. The fit with breaks at distance-dependent energies $E_0(z)$ is better than a fit with any fixed E_b except for a narrow range $E_b \sim (200 - 300)$ GeV.

4 Discussion

In this section, we perform a study of possible systematic effects affecting our results. We will see that the effect we observed cannot be explained by any potential bias or systematics

¹¹For these probability estimates, we assume the chi-squared distribution. The latter is valid for Gaussian errors and can be used here as many independent factors contribute to uncertainties.

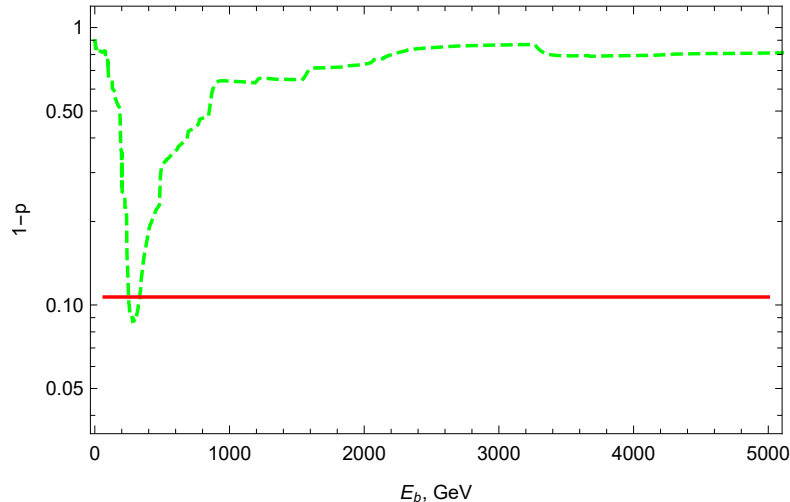


Figure 5. Comparison of the fit quality (good fits correspond to low $(1 - p)$) for the assumptions of spectral breaks at the fixed energy E_b (dashed green line, as a function of E_b) and at the distant-dependent energy $E_0(z)$ (full red line).

we are aware of. Then we compare our result with those of previous studies.

4.1 Systematic uncertainties

4.1.1 Absorption models

The results of the present study may indicate some problems with the absorption model used. For this study, we used the most recent published model by Korochkin and Rubtsov (2018), Ref. [15]. In this section, we repeat our study with several other representative models to see that the effect we found is present independently of the choice of the model. Besides the baseline model of Ref. [15], we considered the following three models:

- (i) Gilmore et al. (2012) fixed [24], used in our previous study [19];
- (ii) Franceschini et al. (2017) [23];
- (iii) a toy upper-limit model normalized to the most recent direct observations of EBL [6, 14].

The latter model was obtained by scaling the model (ii) by a multiplication factor fitted to the data of Refs. [6, 14]. These two independent studies used different techniques to distinguish the extragalactic background light from the foreground contribution: Ref. [6] used spectral templates, which are different for EBL and for foregrounds, while Ref. [14] benefited from observations of an absorbing cloud to separate foregrounds experimentally. Figure 6 presents 15 data points of Ref. [6] and a single data point of Ref. [14] together. All the points, corresponding to different background-light wavelengths, are fitted nicely by the intensity of the model [23] multiplied by a wavelength-independent factor 3.35 ± 0.07 . For

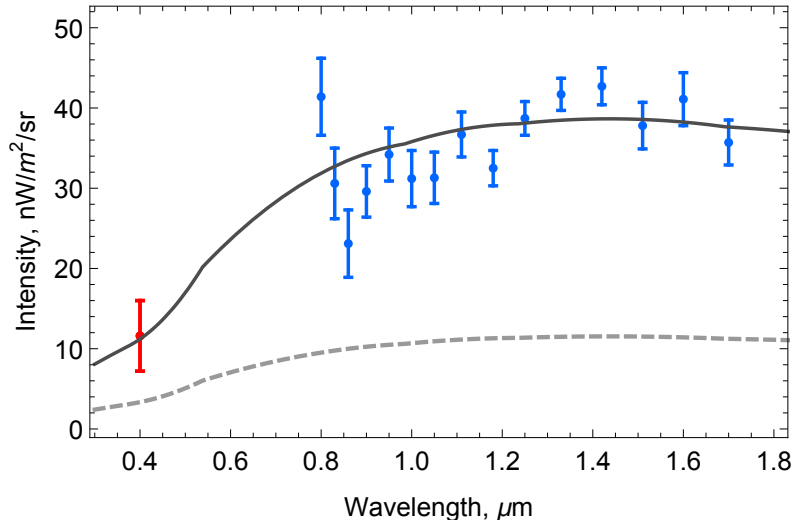


Figure 6. Measurements of the extragalactic background light from Ref. [6] (blue) and Ref. [14] (red, point at 0.4 μm), together with the best-fit scaled intensity of Ref. [23] (full line). This scaling corresponds to the toy upper-limit model used to study systematic uncertainties in Sec. 4.1.1 of this work. The original intensity of Ref. [23] is shown by a dashed line for comparison.

the toy high-absorption model we therefore take the model of Ref. [23] uniformly upscaled by 3.35. The toy absorption model should be considered as an upper limit on the opacity.

As it has been discussed above, the energies E_0 , at which the absorption becomes important, depend on the EBL model, and therefore samples of blazars selected for the study are different for different models. For the models [23, 24], some blazars from Table 1 do not enter the sample while one extra blazar joined the set, see Notes in Table 1. For the toy upper-limit model, the list of 29 sources in the sample is available from the authors by request.

We present the resulting significance of the observation of spectral features at $E_0(z)$ for various absorption models in Table 2. We see that for the low-absorption models, the results are similar to those obtained for the model of Ref. [15]. Clearly, a 3.35 times increase in the opacity, suggested by Refs. [6, 14], had to result in strengthening the effect, and we quantified this consistently within our approach¹².

4.1.2 The Malmquist bias

Given the approach we use (selecting objects detected beyond $\tau = 1$), demonstrating that there is no Malmquist bias is a doable but not-so-easy task. Indeed, inclusion of sources to our sample is limited by observational capabilities of the instruments through the (S2) criterion

¹²The fact that the increase of the absorption up to the values suggested by Ref. [6] sharpens the problems of interpretation of the blazar gamma-ray observations has been illustrated in Ref. [86] for two particular sources.

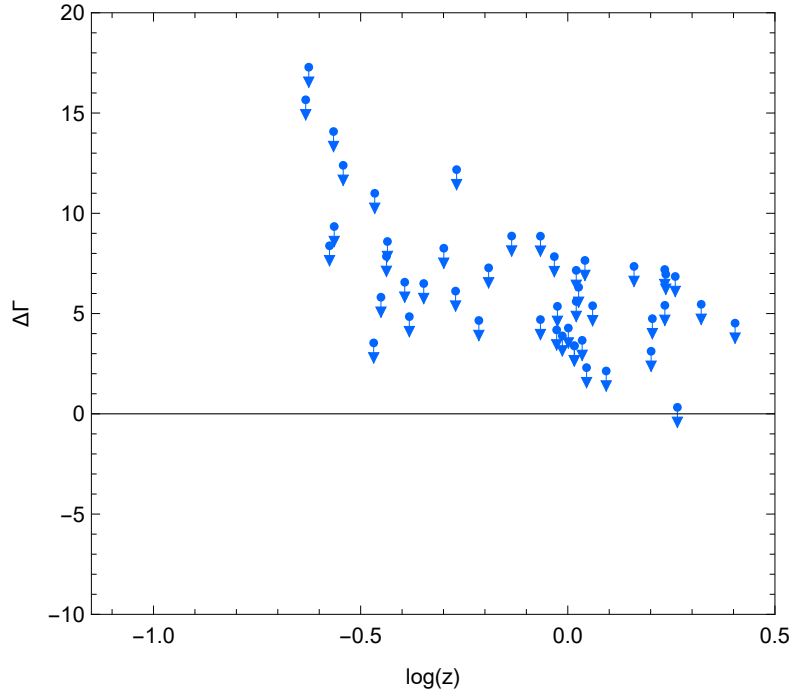


Figure 7. Estimated upper limits (95% CL, downward blue arrows) on the break strength $\Delta\Gamma$ for Fermi-LAT sources not detected at energies above E_0 .

of Sec. 2.1. Therefore, sources intrinsically more and more luminous are included at larger distances. In principle, sources may have spectral features correlated with their luminosity, and the flux selection might mimic the observed effect (a particular model for this is not known). In this hypothetical scenario, weaker objects not detected above E_0 would not have spectral hardenings which we observe for some of the sources included in our sample. This suggests a way to test this possible bias by a study of objects not detected above E_0 .

To this end, we consider the same pre-selected 3FHL sample described in Sec. 2.3 but relax the condition (S2) of Sec. 2.1. Note that we perform the test for Fermi-LAT sources only, not including the sources observed only by IACT. The main reason for the above limitation is that the flux upper limits are not available for the most of the sources observed by IACTs. We obtain a sample of 47 blazars with redshifts between 0.233 and 2.534, which are detected significantly in the spectral bin containing E_0 , but not above. For each of the objects, we determine upper limits on the strength $\Delta\Gamma$ of assumed breaks at E_0 for these sources in the way described in Sec. 3. Following the procedure described in Sec. 2.3 we estimate the Poisson-based flux in the last bins and then calculate 95% CL upper limits on $\Delta\Gamma$. The results of the calculation of these upper limits are presented in Fig. 7. We see that the results obtained with the extended data set do not contradict to those obtained with the main sample, and can conclude that the Malmquist bias does not dominate the results.

4.1.3 Source classes

Gamma-ray sources observed at large distances, the blazars, belong to various classes. In this section, we consider a possibility that distant sources are different from nearby ones, and hence may have systematically different spectral features. In general, broadband spectral energy distributions (SEDs) of blazars have two wide bumps, often associated with the synchrotron and inverse-Compton emissions. Relative positions of the bumps are correlated, which may be explained if the same population of relativistic electrons is responsible for both processes. Therefore, the SEDs are, to the first approximation, characterized by the position of the synchrotron peak so that all blazars form “the blazar sequence” [87]. Flat-spectrum radio quasars (FSRQs) have the synchrotron peak frequency, ν_{peak} , in the radio band, while blazars with ν_{peak} from infrared to X-ray bands represent various subclasses of BL Lac type objects (BLLs). On average, FSRQs are more powerful and less numerous, which results in a potential bias in flux-limited blazar samples: bright FSRQs are seen at large distances while more numerous weaker BLLs dominate the sample at relatively low redshifts. This bias might indeed affect our observations because intrinsic absorption in (distant) FSRQs might introduce spectral features not present in (nearby) BLLs.

The classification of FSRQ or BLL given in Table 1 is based on the information given in the 3FHL catalog for Fermi-LAT sources and in TeVCat for sources observed by IACTs. Since the classification is uncertain and various authors may use different criteria for claiming a source is a FSRQ or a BLL, we obtained approximate values of ν_{peak} for objects in the sample, based on SEDs available in NED and also on Refs. [88–91]. We counted objects with $\nu_{\text{peak}} < 10^{14}$ Hz as FSRQs and others as BLLs, and found that this was in accordance with the classification given in Table 1 for all objects. Fig. 8 demonstrates that the same quantity $\Delta\Gamma$ does not depend on the synchrotron peak frequency. The analyses therefore support the conclusion that potential BLL/FSRQ selection effects described in the beginning of this section are not important. Indirectly, this may suggest that the intrinsic absorption in FSRQs is a subdominant effect with respect to the absorption on EBL.

4.1.4 Tail of the falling spectrum

At the energies under discussion, spectra are determined from event-by-event information about observed individual photons. Determination of the photon energies is subject to statistical and systematic uncertainties. Statistical uncertainties are usually taken into account in the spectrum reconstruction procedures; however, they might be underestimated, while systematics may affect the overall energy scale of an instrument. We are interested in the highest energies, where, because of steeply falling spectra, the flux is often estimated from observations of a few photons only. In the case of a systematic shift of their energies upwards,

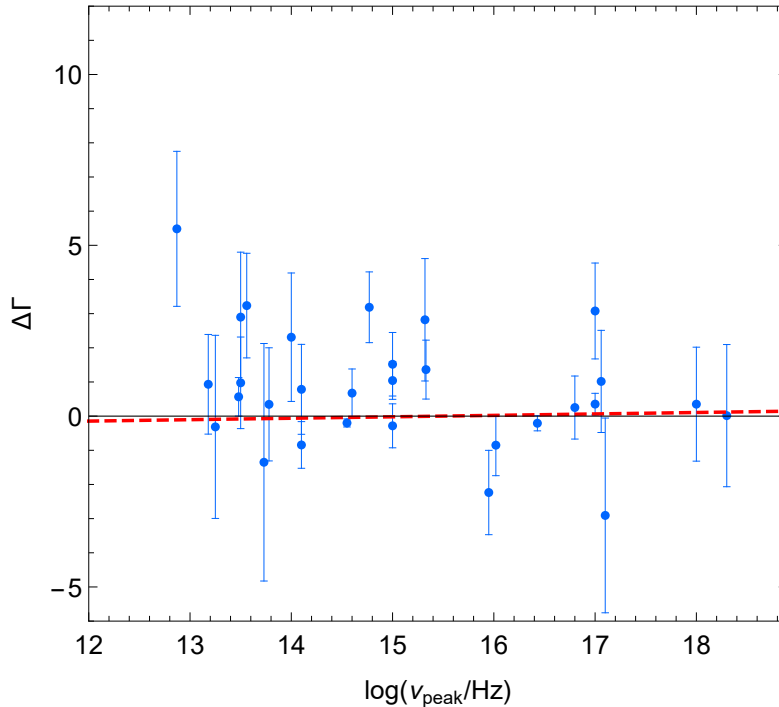


Figure 8. Breaks in the deabsorbed spectra of blazars versus the approximate synchrotron peak frequency.

or if the statistical uncertainty is larger than expected, overestimation of the energies of these few photons may affect significantly the shape of the spectrum.

We first address potential systematic errors. These are instrument-dependent, and we take advantage of having objects observed by four different instruments in our sample. Table 3 presents significances of the observed distance-dependent spectral hardenings in subsamples of objects with data of one of the instruments dropped. The observed significance is stable and agrees well with the expectations from the sample size. Therefore, only a coherent upward systematic error in the energy estimation by the three IACTs and Fermi LAT may result in the effect we found. We note that this situation is unlikely.

We turn now to the possibility of underestimated statistical errors, which may result in occasional overestimation of energies of particular photons. In the case of the published spectra, this effect is normally already taken into account by the observing collaboration by making use of the “unfolding” procedure, see e.g. Ref. [92]. In any case, this potential systematics would be strongly suppressed for the objects where the spectral hardening happens at energies for which a sufficient number of photons is observed. To select those from our sample, we replace the (S2) selection criterion from Sec. 2.1 by a much stronger one, requiring two (instead of one) spectral bins above E_0 . We stress that this does not directly select objects observed at larger optical depths, nor intrinsically brighter sources; this just

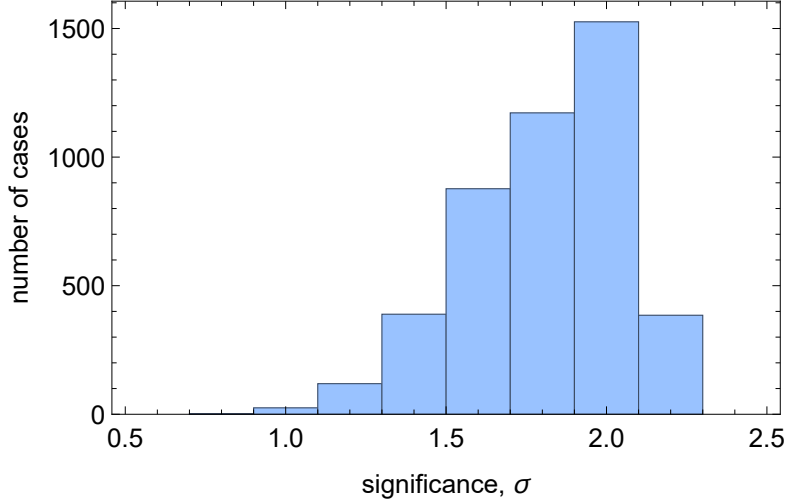


Figure 9. Distribution of significances for the samples with 2 objects artificially removed, imitating potential wrong redshifts.

reduces statistical errors in the determination of $\Delta\Gamma$. Only 17 of 31 objects in our sample satisfy this criterion. Performing our analysis for these 17 objects, we find the significance of $\sim 2.7\sigma$ for this purified sample. This disfavors the relation of our observation to potentially underestimated errors in the energy determination; moreover, the fact that a purified, though depleted, sample exhibits a somewhat stronger effect supports its physical origin.

4.1.5 Redshifts

Our study of distance-dependent spectral features is sensitive to correct determination of distances to the sources. However, redshifts of distant blazars are not always determined unambiguously. In particular (see Sec. 4.2), redshifts of 4 of 20 objects in the sample we used for our previous study [19] in 2014 were found to be unreliable by 2018, and the objects left our present sample. Though for the present sample we performed a careful selection of objects based on the quality of their redshifts, see criteria (R1), (R2 x) in Sec. 2.1, one might imagine that some of the 31 redshifts would still appear wrong in future analyses. To understand how this might affect our results, we artificially removed 1, 2 or 3 objects in all possible combinations from the sample and repeated our analysis with the reduced samples. With 1 object removed, the lowest significance was 1.5σ and the highest one was 2.0σ ; for 2 objects removed the interval was $(1.1 \div 2.1)\sigma$; for 3 objects removed it was $(0.8 \div 2.2)\sigma$. Figure 9 presents the distribution of significances among samples with 2 objects removed. We see that while it is possible to select sources from the sample whose removal would have a significant impact on the result, in most cases this is not expected.

4.2 Comparison to previous studies

In this section, we give a detailed comparison of our methods and results with those of key previous studies of the gamma-ray opacity of the Universe with ensembles of blazar spectra.

4.2.1 Rubtsov and Troitsky (2014) [19]

The present work follows the same approach as our previous work [19]. Advantages of the present work, besides the use of new observational data and a more detailed report on systematics, are:

(i) pre-selection of Fermi-LAT sources with the 3FHL catalog and the use of Pass 8 data processing;

(ii) use of new conservative EBL models [15, 23];

(iii) imposing strict criteria on the redshift quality;

(iv) use of a more conservative method which is not based on the bin-by-bin deabsorption;

(v) use of a more general statistical test of the presence of spectral breaks.

For the point (v), we stress here that the null hypothesis to be tested is the absence of any spectral features at $E_0(z)$. This hypothesis is disfavoured at 1.9σ in the present work. In Ref. [19], we observed the linear growth of $\Delta\Gamma$ with $\log z$, which does not have a known physical model behind it.

Next, the changes in criteria resulted in the removal of 5 sources from the sample of Ref. [19]: redshifts of 3 objects (RGB J1448+361, 1ES 1101–232 and 1ES 0347–121) did not satisfy our new quality criteria; the reported value of the redshift of B3 1307+433 changed in such a way that the object no longer satisfies the (S2) criterion; for PKS J0730–1141, new Pass 8 Fermi-LAT reconstruction does not result in a significant detection at $E > E_0$, contrary to the Pass 7REP (V15) used in Ref. [19]. Removal of the most distant objects from the sample, together with a more conservative analysis method, resulted in a considerable reduction of the resulting significance (was 12.4σ for the linear-growth test, now 1.9σ for the exclusion of the null hypothesis).

It is interesting to note that the present study does not confirm the linear growth of spectral breaks with $\log z$ observed in Ref. [19] and never explained theoretically within any approach. Figure 10 demonstrates that the significant distance dependence observed earlier was dominated by the effect of distant sources whose redshifts do not pass the quality cuts applied in the present study. Better measurements of redshifts of distant blazars observed in VHE gamma rays are clearly welcome.

4.2.2 Horns and Meyer (2012) [18]

Ref. [18] was the first study addressing quantitatively spectral hardenings in the ensemble of distant gamma-ray sources.

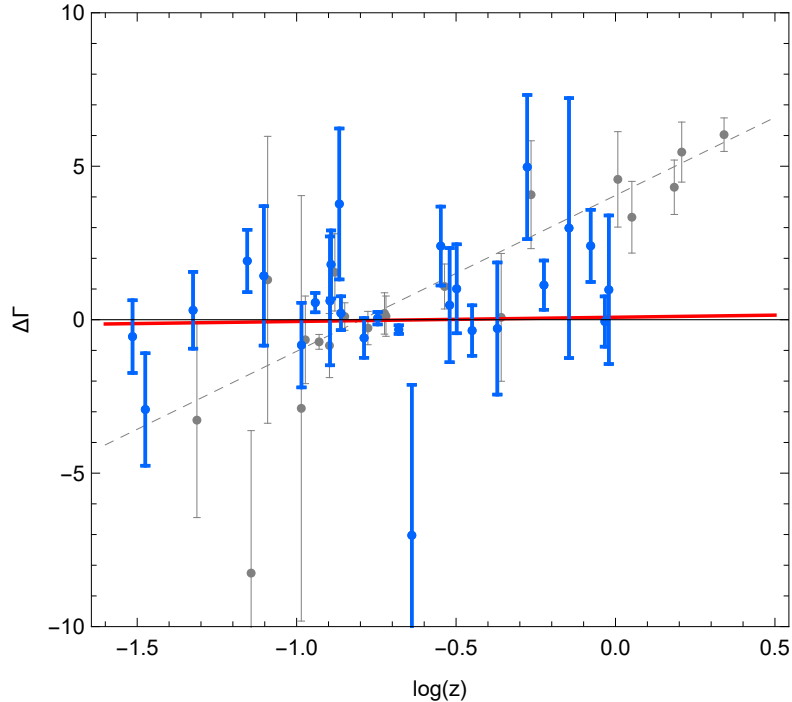


Figure 10. Comparison of the present result with that of Ref. [19]: spectral breaks at $E_0(z)$ in deabsorbed (model of Gilmore et al. (2012) fixed) blazar spectra versus redshift. Individual data points for objects in the sample studied in the present work are shown in blue (thick error bars); the full red line represents the best fit of $\Delta\Gamma$ as a linear function in $\log z$. Data points of Ref. [19] are shown in gray (thin error bars), slightly shifted to the right for clarity; the corresponding best fit of Ref. [19] is presented as a thin dashed line.

(1) Both Ref. [18] and our study address upward spectral breaks at distance-dependent energies.

(2) Only objects observed by IACTs ($z < 0.536$) were included in the sample of Ref. [18]. There, a stricter requirement of detection at optical depths $\tau > 2$ was used, resulting in the sample of 7 objects only, while we require $\tau > 1$ and include objects for which the break was not significantly detected.

(3) In Ref. [18], bin-by-bin deabsorption was used but the correction for the mean energy in the bin for deabsorption was not implemented.

4.2.3 Fermi-LAT collaboration (2012) [13]

The interesting work [13] presented an analysis of the ensemble of BLLs detected by Fermi LAT at high redshifts and, for the first time, presented a detection of the EBL absorption in stacked spectra of these distant sources. The ensemble of 150 BLLs with redshifts $\lesssim 1.6$ was split into three distance bins, and intrinsic spectra were extrapolated from Fermi-LAT

observations at low energies. The EBL absorption correction was subsequently determined from spectra stacked within the three redshift bins.

As we know from our present study, only a few blazars (5 with our criteria) have been confidently observed by Fermi LAT above E_0 . Constraints on the amount of absorption obtained in Ref. [13] were not very tight. While available absorption models are consistent with the upper part of the allowed band in $\tau(E)$ for $z = 1$, cf. Fig. 1 of Ref. [13], considerably lower absorption is allowed for all energies. This is in agreement with our results.

4.2.4 Biteau and Williams (2015) [11]

Ref. [11] considered 106 spectra of 38 sources observed by IACTs. Every spectrum was deabsorbed bin-by-bin, without applying the correction for the mean energy of the bin, and then fitted by a model spectrum for which a concave shape was assumed. This study did not reveal any anomaly in the absorption on EBL.

We argue that nonobservation of the absorption anomaly in Ref. [11] does not contradict to the results of the present work. The difference in conclusions is related both to the sample of source spectra used and to the assumptions on the intrinsic spectra. We point out the following differences:

1. In the sample of Ref. [11], a different set of sources is used, dominated by nearby ones, while the observation of anomalous features at various $E_0(z)$ requires a good redshift coverage. The dominance of nearby sources in Ref. [11] was enhanced by the use of multiple spectra per source, which gave higher statistical weights to better studied nearby objects, see Figure 11. Different spectra of the same objects were treated as independent data in the statistical analysis of Ref. [11], which may introduce statistical biases.
2. The individual-source analysis of Ref. [11] assumed explicitly a concave shape for the deabsorbed spectrum, thus not allowing for the hardenings we study here by construction, see Figure 12. In fact, in most cases (91 of 106 spectra, in particular for all sources with $z > 0.12$), the best-fit model corresponded to a power law, that is to the margin of the allowed concave spectra: convex shapes, which give better fits for many of the spectra in our study, were not allowed.

We conclude that the methods chosen by Biteau and Williams in Ref. [11] are insensitive to the anomalous effects found in Refs. [18, 19] and studied here, therefore Ref. [11] and our work are not in a contradiction.

In addition to the main study, which did not allow for convex spectra by definition, Biteau and Williams addressed the result of Horns and Meyer [18] discussed above. While they

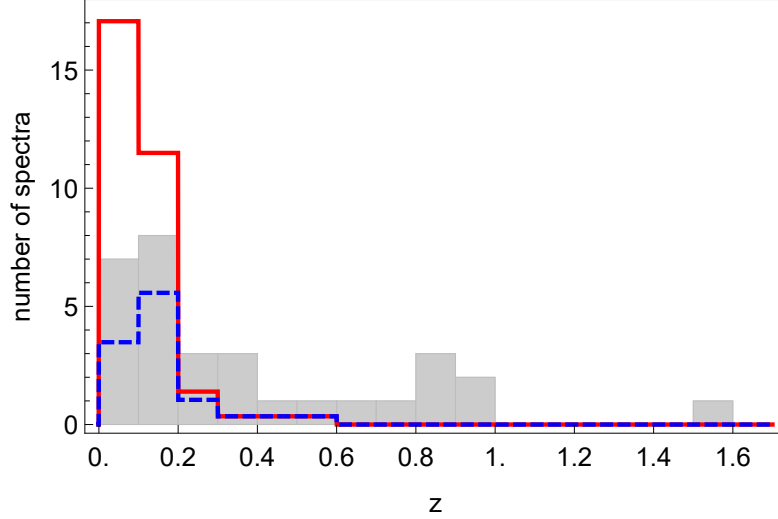


Figure 11. Comparison of the redshift coverage of the sample used by Biteau and Williams [11] and of our sample. Red full line: distribution of redshifts for individual spectra used in the analysis of Ref. [11] (uncertain, lower-limit and erroneous redshifts are not included). Blue dashed line: independent (one spectrum per source) spectra from Ref. [11]. Shaded histogram: redshifts in our sample. Red line and shaded histogram are normalized to the total number of spectra used, blue line gives a fraction of the red-line distribution.

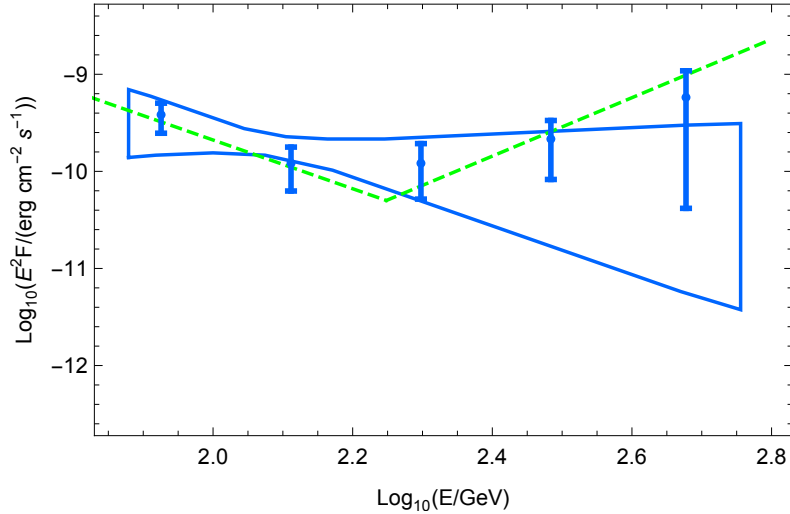


Figure 12. Comparison of the treatment of a single binned spectrum by Biteau and Williams [11] and in the present work, using 3C 279 (spectrum from Ref. [40]) as an example. Data points: deabsorbed spectrum from Ref. [11], flux data points attributed to median log observed energy of the bins. The blue butterfly gives the allowed range of *concave* spectra of Ref. [11] while the dashed green line represents our best-fit spectrum which assumes the break at $E_0(z)$ for $z = 0.536$, the redshift of 3C 279.

confirmed that the application of the method of Horns and Meyer to their sample results in a significant dependence of the break position on the redshift (with even stronger significance than in the original Ref. [18]), Biteau and Williams claimed that the reason for the effect found in Ref. [18] was in incorrect treatment of statistical uncertainties of the flux measurements: the method of Horns and Meyer, based on a nonparametric Kolmogorov–Smirnov test¹³, does not take the uncertainties into account and is sensitive to central values of the measured flux only. To illustrate this, Biteau and Williams searched for observed excesses in residuals over best-fit concave spectra at energies corresponding to large optical depths. The results of the analysis, performed for their full set of spectra, indicated no significant deviations. This part of the study [11], however, also suffers from the use of multiple spectra of the same objects treated as statistically independent data. In addition, these residuals were calculated with respect to the best-fit spectra deabsorbed with the EBL model determined from the very same spectra, which makes the problem of independent treatment of data points even more complicated.

4.2.5 Galanti et al. (2015) [93]

It is interesting to note that distance-dependent hardenings can still be noticed with the analysis based on a single power-law fit. Galanti et al. (2015) [93] considered a sample of 39 blazars observed by IACTs ($z \leq 0.536$), for all tested opacities. Deabsorbed spectra were described by single power laws, and the distance dependence of the spectral index was studied. Though this approach does not constructively include spectral breaks, deabsorbed spectra with upward breaks look harder when fitted by a power-law, and this hardness was found to be redshift-dependent. Therefore, results of Ref. [93] are in agreement with Ref. [19].

4.2.6 Studies of high-energy versus very-high-energy spectral indices

Several previous studies used as their observables the difference between spectral indices in the high-energy (roughly, GeV; definition varies) and very-high-energy (roughly, hundreds of GeV) bands. These works include Stecker et al. (2006) [94], Stecker and Scully (2010) [95], Sanchez et al. (2013) [96], Essey and Kusenko (2012) [97]. The most elaborated study of this kind, Dominguez and Ajello (2015) [98], was based entirely on the Fermi-LAT data and was therefore insensitive to relative systematic errors of the energy determination by different experiments. It was also the only one working with spectra corrected for the absorption on EBL. In all these studies, the energy of spectral breaks was a priori fixed to a certain value, uniform for all sources. Therefore, the results of the papers mentioned, some of which pointed to anomalies, some did not, cannot be directly compared to ours, because we assumed breaks at energies $E_0(z)$, different for different sources.

¹³Ref. [11] mentions the Anderson–Darling method which was not used to obtain the main result of Ref. [18].

5 Conclusions

In the present work, we readdress the problem of the anomalous transparency of the Universe for high-energy gamma rays, the most significant indications to which [18, 19] were based on unphysical spectral features in deabsorbed spectra for an ensemble of blazars which showed up precisely at the energies for which the correction for the absorption on EBL became important. By making use of a more robust analysis procedure which avoids bin-by-bin deabsorption and tests only the null hypothesis, of new gamma-ray and redshift data and of most recent EBL models, we disfavour the absence of anomalous distance-dependent spectral features with the modest statistical significance of 1.9σ . At the same time we do not confirm the linear dependence of the break strength with $\log z$. We discuss potential biases and systematic errors and, by performing various tests, conclude that they cannot seriously affect our results.

Interpretations of the anomalous transparency of the Universe have been widely discussed in the literature, see e.g. Ref. [99] for a brief review and a list of references. The simplest possible culprit for unphysical spectral features might be an overestimated EBL intensity. However, reduction of the intensity below the levels predicted by the models we use might be dangerous because the model intensities are very close to the lower limits from galaxy counting. With the help of the Markov-chain optimization behind the model [15], we plan to attempt to change the EBL model in such a way that the effect, hints to which we observe in the present work, is absent and to understand how much in conflict this would be with underlying astrophysical data. This will be a subject of a forthcoming work.

A number of proposals attempted to explain the apparent anomalous transparency of the Universe by adding secondary emission to that arriving directly from the source. If these secondary photons are born relatively close to the observer, they do not have time to produce e^+e^- pairs and arrive unattenuated. With respect to the origin of this secondary emission, it is useful to distinguish the cases when it is caused by electromagnetic cascades [100] or from interactions of hadronic cosmic-ray particles [101, 102]. The main characteristic feature of both approaches is that they require extremely low magnetic fields all along the propagation path of the cascade, otherwise secondary photons would not point to the sources because of deflections of their progenitor charged particles in the cascade.

Other proposals require modification of the photon interactions. We note that the pair-production cross section has been well determined experimentally, and the only possibility to change it in the kinematic regimes relevant for our study is to allow for small deviations from the Lorentz invariance. However, this change would affect also the development of photon-induced atmospheric showers [103, 104] making the work of IACTs impossible, so that the scenario, in which results of Sec. 3 are explained by the Lorentz-invariance violation, is in fact excluded by the fact that some high-energy photons have been detected by these instruments

(see also Ref. [105]). The remaining explanation invokes a hypothetical axion-like particle (ALP). In external magnetic fields, ALP mixes with photons [106] and, since ALP does not attenuate on EBL, this makes it possible to detect photons from more distant sources. In one of the scenarios, this mixing takes place in intergalactic magnetic fields along the path from the source to the observer [107, 108], while in the other, a part of photons is converted to ALPs near the source and reconverted back to gamma rays in our neighbourhood (in the magnetic fields of galaxies, clusters and filaments) [109, 110]. Observational consequences of the two scenarios are compared to each other and to data in Ref. [111]. The account of interactions of energetic photons with the axion-like particle allows one to explain consistently all indications to the anomalous transparency of the Universe without contradicting to any other experimental or observational data. Our present results indicate that further studies are required to prove or exclude the need for new-physics effects in the propagation of energetic gamma rays through the Universe.

A Observed and best-fit intrinsic spectra of blazars in the main sample.

Figures 13–16 present the observed and deabsorbed spectra of 31 blazars from our main sample, see Table 1, together with values of E_0 and break strengths $\Delta\Gamma$ on which the main result of the paper is based. The observed spectra and numerical values of spectral breaks are available online as a supplementary material for this paper.

Acknowledgments

This research has made use of the NASA/IPAC Extragalactic Database (NED), which is operated by the Jet Propulsion Laboratory, California Institute of Technology, under contract with the National Aeronautics and Space Administration. This research has made use of the TeVcat online source catalog [27] and of the data and tools provided by the Fermi Science Support Center.

We are indebted to Alberto Franceschini for interesting correspondence and for sharing detailed numerical tables of the absorption model [23] with us; to Manuel Meyer for numerous interesting discussions and helpful comments; to Timur Dzhatdov, Oleg Kalashev, Mikhail Kuznetsov, Maxim Libanov, Valery Rubakov and Igor Tkachev for interesting discussions. We thank the anonymous reviewer for careful reading of the manuscript and the attention to the study which went beyond the usual referee’s duties. The work of AK and ST on constraining the intensity of EBL and its applications to astrophysical manifestations of axion-like particles was supported by the Russian Science Foundation, grant 18-12-00258.

Note added. Several months after this study was completed and submitted, an update of Ref. [13] was published by the Fermi LAT Collaboration [112]. We will compare our results to those of Ref. [112] in a forthcoming publication based on Fermi-LAT data only.

References

- [1] A.I. Nikishov, *Absorption of high-energy photons in the Universe*, *Sov. Phys. JETP* **14** (1962) 393 [*ZhETF* **41** (1962) 549].
- [2] K. Sano, K. Kawara, S. Matsuura, H. Kataza, T. Arai and Y. Matsuoka, *Derivation of a large isotropic diffuse sky emission component at 1.25 and 2.2 μ m from the COBE/DIRBE data*, *Astrophys. J.* **811** (2015) 77 [arXiv:1508.02806 [astro-ph.GA]].
- [3] K. Sano, K. Kawara, S. Matsuura, H. Kataza, T. Arai and Y. Matsuoka, *Measurements of Diffuse Sky Emission Components in High Galactic Latitudes at 3.5 and 4.9 μ m Using DIRBE and WISE Data*, *Astrophys. J.* **818** (2016) 72 [arXiv:1512.08072 [astro-ph.GA]].
- [4] T. Matsumoto, M. G. Kim, J. Pyo and K. Tsumura, *Reanalysis of the near-infrared extragalactic background light based on the IRTS Observations*, *Astrophys. J.* **807** (2015) 57 [arXiv:1501.01359 [astro-ph.GA]].
- [5] K. Tsumura, T. Matsumoto, S. Matsuura, I. Sakon and T. Wada, *Low-Resolution Spectrum of the Extragalactic Background Light with AKARI InfraRed Camera*, *Publ. Astron. Soc. Jap.* **65** (2013) 121 [arXiv:1307.6740 [astro-ph.CO]].
- [6] S. Matsuura *et al.*, *New Spectral Evidence of an Unaccounted Component of the Near-infrared Extragalactic Background Light from the CIBER*, *Astrophys. J.* **839** (2017) 7 [arXiv:1704.07166 [astro-ph.GA]].
- [7] P. Madau and L. Pozzetti, *Deep galaxy counts, extragalactic background light, and the stellar baryon budget*, *Mon. Not. Roy. Astron. Soc.* **312** (2000) L9 [astro-ph/9907315].
- [8] S. P. Driver *et al.*, *Measurements of Extragalactic Background Light From the far UV to the far IR From Deep Ground- and Space-based Galaxy Counts*, *Astrophys. J.* **827** (2016) 108 [arXiv:1605.01523 [astro-ph.GA]].
- [9] R. C. Keenan, A. J. Barger, L. L. Cowie, W. H. Wang, *The Resolved Near-infrared Extragalactic Background* *Astrophys. J.* **723** (2010) 40.
- [10] M. L. Ahnen *et al.*, *MAGIC observations of the February 2014 flare of 1ES 1011+496 and ensuing constraint of the EBL density*, *Astron. Astrophys.* **590** (2016) A24 [arXiv:1602.05239 [astro-ph.HE]].
- [11] J. Biteau and D. A. Williams, *The extragalactic background light, the Hubble constant, and anomalies: conclusions from 20 years of TeV gamma-ray observations*, *Astrophys. J.* **812** (2015) 60 [arXiv:1502.04166 [astro-ph.CO]].

- [12] A. Abramowski *et al.* [H.E.S.S. Collaboration] *Measurement of the extragalactic background light imprint on the spectra of the brightest blazars observed with H.E.S.S.* *Astron. Astrophys.* **550** (2013) 11.
- [13] M. Ackermann *et al.* [Fermi-LAT Collaboration], *The Imprint of The Extragalactic Background Light in the Gamma-Ray Spectra of Blazars*, *Science* **338** (2012) 1190 [arXiv:1211.1671 [astro-ph.CO]].
- [14] K. Mattila, P. Vaisanen, K. Lehtinen, G. von Appen-Schnur, Ch. Leinert, *Extragalactic background Light: a measurement at 400 nm using dark cloud shadow II. Spectroscopic separation of dark cloud's light, and results*, *Mon. Not. Roy. Astron. Soc.* **470** (2017) 2152 [arXiv:1705.10790 [astro-ph.GA]].
- [15] A. A. Korochkin and G. I. Rubtsov, *Constraining the star formation rate with the extragalactic background light*, *Mon. Not. Roy. Astron. Soc.* **481** (2018) 557 [arXiv:1712.06579 [astro-ph.GA]].
- [16] R. J. Protheroe and H. Meyer, *An Infrared background TeV gamma-ray crisis?*, *Phys. Lett. B* **493** (2000) 1 [astro-ph/0005349].
- [17] F. Aharonian, D. Khangulyan and L. Costamante, *Formation of hard VHE gamma-ray spectra of blazars due to internal photon-photon absorption*, *Mon. Not. Roy. Astron. Soc.* **387** (2008) 1206 [arXiv:0801.3198 [astro-ph]].
- [18] D. Horns and M. Meyer, *Indications for a pair-production anomaly from the propagation of VHE gamma-rays*, *JCAP* **1202** (2012) 033 [arXiv:1201.4711 [astro-ph.CO]].
- [19] G. I. Rubtsov and S. V. Troitsky, *Breaks in gamma-ray spectra of distant blazars and transparency of the Universe*, *JETP Lett.* **100** (2014) 355 [*Pisma Zh. Eksp. Teor. Fiz.* **100** (2014) 397] [arXiv:1406.0239 [astro-ph.HE]].
- [20] W. Atwood *et al.* [Fermi-LAT Collaboration], *Pass 8: Toward the Full Realization of the Fermi-LAT Scientific Potential*, arXiv:1303.3514 [astro-ph.IM].
- [21] M. Ajello *et al.* [Fermi-LAT Collaboration], *3FHL: The Third Catalog of Hard Fermi-LAT Sources*, *Astrophys. J. Suppl.* **232** (2017) 18 [arXiv:1702.00664 [astro-ph.HE]].
- [22] F. W. Stecker, S. T. Scully and M. A. Malkan, *An Empirical Determination of the Intergalactic Background Light from UV to FIR Wavelengths Using FIR Deep Galaxy Surveys and the Gamma-ray Opacity of the Universe*, *Astrophys. J.* **827** (2016) 6 [Erratum: *Astrophys. J.* **863** (2018) 112] [arXiv:1605.01382 [astro-ph.HE]].
- [23] A. Franceschini and G. Rodighiero, *The extragalactic background light revisited and the cosmic photon-photon opacity*, *Astron. Astrophys.* **603** (2017) A34 [arXiv:1705.10256 [astro-ph.HE]]. Erratum: *Astron. Astrophys.* **614** (2018) C1.
- [24] R. C. Gilmore, R. S. Somerville, J. R. Primack and A. Dominguez, *Semi-analytic modeling of the EBL and consequences for extragalactic gamma-ray spectra*, *Mon. Not. Roy. Astron. Soc.* **422** (2012) 3189 [arXiv:1104.0671 [astro-ph.CO]].

- [25] M. Colless *et al.* [2DFGRS Collaboration], *The 2dF Galaxy Redshift Survey: Spectra and redshifts*, *Mon. Not. Roy. Astron. Soc.* **328** (2001) 1039 [astro-ph/0106498].
- [26] D. H. Jones *et al.*, *The 6dF Galaxy Survey: Final Redshift Release (DR3) and Southern Large-Scale Structures*, *Mon. Not. Roy. Astron. Soc.* **399** (2009) 683 [arXiv:0903.5451 [astro-ph.CO]].
- [27] S. P. Wakely and D. Horan, *TeVcat: An online catalog for Very High Energy Gamma-Ray Astronomy*, Proc. 30th International Cosmic Ray Conference, Mexico (2004) **3**, 1341. Available at <http://tevcat.uchicago.edu>.
- [28] W. B. Atwood *et al.* [Fermi-LAT Collaboration], *The Large Area Telescope on the Fermi Gamma-ray Space Telescope Mission*, *Astrophys. J.* **697** (2009) 1071 [arXiv:0902.1089 [astro-ph.IM]].
- [29] F. Acero *et al.* [Fermi-LAT Collaboration], *Fermi Large Area Telescope Third Source Catalog*, *Astrophys. J. Suppl.* **218** (2015) 23 [arXiv:1501.02003 [astro-ph.HE]].
- [30] M. S. Shaw *et al.*, *Spectroscopy of The Largest Ever Gamma-ray Selected BL Lac Sample*, *Astrophys. J.* **764** (2013) 135 [arXiv:1301.0323 [astro-ph.HE]].
- [31] M. S. Shaw *et al.*, *Spectroscopy of Broad Line Blazars from 1LAC*, *Astrophys. J.* **748** (2012) 49 [arXiv:1201.0999 [astro-ph.HE]].
- [32] M. L. Ahnen *et al.* [MAGIC and Fermi-LAT Collaborations], *Very-high-energy gamma-rays from the Universe's middle age: detection of the $z = 0.940$ blazar PKS 1441+25 with MAGIC*, *Astrophys. J.* **815** (2015) L23 [arXiv:1512.04435 [astro-ph.GA]].
- [33] D. P. Schneider *et al.* [SDSS Collaboration], *The Sloan Digital Sky Survey Quasar Catalog. 3. Third data release*, *Astron. J.* **130** (2005) 367 [astro-ph/0503679].
- [34] B. A. Peterson *et al.*, *Redshifts of southern radio sources*, *Astrophys. J.* **207** (1975) L5.
- [35] K. N. Abazajian *et al.* [SDSS Collaboration], *The Seventh Data Release of the Sloan Digital Sky Survey*, *Astrophys. J. Suppl.* **182** (2009) 543 [arXiv:0812.0649 [astro-ph]].
- [36] T. Terzic *et al.*, *First detection of VHE gamma-ray signal from the FSRQ TON 0599, TeVPA-2018*, available at: <https://indico.desy.de/indico/event/18204/session/16/contribution/248/material/slides/0.pdf>
- [37] P. C. Hewett and V. Wild, *Improved redshifts for SDSS quasar spectra*, *Mon. Not. Roy. Astron. Soc.* **405** (2010) 2302 [arXiv:1003.3017 [astro-ph.CO]].
- [38] V. A. Acciari *et al.* [VERITAS and Fermi Collaborations], *Discovery of very high energy gamma rays from PKS 1424+240 and multiwavelength constraints on its redshift*, *Astrophys. J.* **708** (2010) L100 [arXiv:0912.0730 [astro-ph.CO]].
- [39] S. Paiano *et al.*, *On the Redshift of TeV BL Lac Objects*, *Astrophys. J.* **837** (2017) 144 [arXiv:1701.04305 [astro-ph.GA]].

- [40] E. Aliu *et al.* [MAGIC Collaboration], *Very-High-Energy Gamma Rays from a Distant Quasar: How Transparent Is the Universe?*, *Science* **320** (2008) 1752 [arXiv:0807.2822 [astro-ph]].
- [41] P. Marziani *et al.*, *Comparative Analysis of the High- and Low-Ionization Lines in the Broad-Line Region of Active Galactic Nuclei*, *Astrophys. J. Suppl. Ser.* **104** (1996) 37
- [42] J. Aleksic *et al.* [MAGIC Collaboration], *MAGIC discovery of VHE Emission from the FSRQ PKS 1222+21*, *Astrophys. J.* **730** (2011) L8 [arXiv:1101.4645 [astro-ph.HE]].
- [43] D. E. Osterbrock, R. W. Pogge, *Optical spectra of narrow emission line Palomar-Green galaxies*, *Astrophys. J.* **323** (1987) 108.
- [44] V. A. Acciari *et al.* [MAGIC and Fermi-LAT Collaborations], *Detection of persistent VHE gamma-ray emission from PKS 1510-089 by the MAGIC telescopes during low states between 2012 and 2017*, *Astron. Astrophys.* **619** (2018) A159 [arXiv:1806.05367 [astro-ph.GA]].
- [45] D. J. Thompson, S. Djorgovski, R. de Carvalho, *Spectroscopy of radio sources from the Parkes 2700 MHz survey*, *Publ. Astron. Soc. Pacific* **102** (1990) 1235.
- [46] F. Schussler *et al.* [H.E.S.S. Collaboration], *Target of Opportunity Observations of Blazars with H.E.S.S.*, *PoS ICRC 2017* (2018) 652 [arXiv:1708.01083 [astro-ph.HE]].
- [47] M. Stickel, J. W. Fried, H. Kuehr. *The redshifts of the BL Lac objects 1749+096 and 2254+074*, *Astron. Astrophys.* **191** (1988) L16.
- [48] S. O'Brien [VERITAS Collaboration], *VERITAS detection of VHE emission from the optically bright quasar OJ 287*, *PoS ICRC 2017* (2018) 650 [arXiv:1708.02160 [astro-ph.HE]].
- [49] K. Nilsson, L. O. Takalo, H. J. Lehto and A. Sillanpaa, *H-alpha monitoring of OJ 287 in 2005-08*, *Astron. Astrophys.* **516** (2010) A60 [arXiv:1004.2617 [astro-ph.CO]].
- [50] A. Abramowski *et al.* [H.E.S.S. Collaboration], *Discovery of hard-spectrum γ -ray emission from the BL Lac object 1ES 0414+009*, *Astron. Astrophys.* **538** (2012) A103 [arXiv:1201.2044 [astro-ph.HE]].
- [51] J. P. Halpern *et al.*, *The redshift of the X-ray selected BL Lacertae object H0414+009*, *Astron. J.* **101** (1991) 818.
- [52] F. Gate *et al.* [H.E.S.S. Collaboration], *H.E.S.S. observations of very-high-energy emission from 1RXS J023832.6–311658*, *PoS ICRC 2017* (2018) 645 [arXiv:1708.09612 [astro-ph.HE]].
- [53] M. L. Ahnen *et al.*, *MAGIC observations of the February 2014 flare of 1ES 1011+496 and ensuing constraint of the EBL density*, *Astron. Astrophys.* **590** (2016) A24 [arXiv:1602.05239 [astro-ph.HE]].
- [54] J. Albert *et al.* [MAGIC Collaboration], *Discovery of Very High Energy gamma-rays from 1ES1011+496 at $z = 0.212$* , *Astrophys. J.* **667** (2007) L21 [arXiv:0706.4435 [astro-ph]].
- [55] A. S. Madhavan [VERITAS Collaboration], *VERITAS Long-Term Observations of Hard Spectrum Blazars*, arXiv:1307.7051 [astro-ph.HE].

- [56] C. P. Ahn *et al.* [SDSS Collaboration], *The Ninth Data Release of the Sloan Digital Sky Survey: First Spectroscopic Data from the SDSS-III Baryon Oscillation Spectroscopic Survey*, *Astrophys. J. Suppl.* **203** (2012) 21 [arXiv:1207.7137 [astro-ph.IM]].
- [57] A. Abramowski *et al.* [H.E.S.S. Collaboration], *Multi-wavelength Observations of H 2356–309*, *Astron. Astrophys.* **516** (2010) A56 [arXiv:1004.2089 [astro-ph.HE]].
- [58] T. Fang *et al.*, *An HST/COS Observation of Broad Ly α Emission and Associated Absorption Lines of the BL Lacertae Object H 2356-309*, *Astrophys. J.* **795** (2014) 57 [arXiv:1409.6432 [astro-ph.GA]].
- [59] E. Aliu *et al.*, *A three-year multi-wavelength study of the very-high-energy γ -ray blazar 1ES 0229+200*, *Astrophys. J.* **782** (2014) 13 [arXiv:1312.6592 [astro-ph.HE]].
- [60] J. F. Schachter *et al.*, *Ten new BL Lacertae objects discovered by an efficient X-ray/radio/optical technique*, *Astrophys. J.* **412** (1993) 541.
- [61] J. Aleksic *et al.* [MAGIC Collaboration], *MAGIC detection of short-term variability of the high-peaked BL Lac object 1ES 0806+524*, *Mon. Not. Roy. Astron. Soc.* **451** (2015) 739 [arXiv:1504.06115 [astro-ph.GA]].
- [62] M. Trichas *et al.*, *The Chandra Multi-Wavelength Project: Optical Spectroscopy and the Broadband Spectral Energy Distributions of X-ray Selected AGN*, *Astrophys. J. Suppl.* **200** (2012) 17 [arXiv:1204.5148 [astro-ph.CO]]. Erratum: *Astrophys. J. Suppl.* **231** (2017) 23.
- [63] J. Aleksic *et al.* [MAGIC Collaboration], *Discovery of VHE gamma-rays from the blazar 1ES 1215+303 with the MAGIC Telescopes and simultaneous multi-wavelength observations*, *Astron. Astrophys.* **544** (2012) A142 [arXiv:1203.0490 [astro-ph.HE]].
- [64] D. Horns *et al.* [HEGRA Collaboration], *TeV observations of H1426+428 with HEGRA*, *New Astron. Rev.* **48** (2004) 387.
- [65] R. M. Plotkin *et al.*, *Optically Selected BL Lacertae Candidates from the Sloan Digital Sky Survey Data Release Seven*, *Astron. J.* **139** (2010) 390 [arXiv:0911.0423 [astro-ph.CO]].
- [66] A. Abramowski *et al.* [H.E.S.S. Collaboration], *VHE gamma-ray emission of PKS 2155-304: spectral and temporal variability*, *Astron. Astrophys.* **520** (2010) A83 [arXiv:1005.3702 [astro-ph.HE]].
- [67] R. Falomo, J. E. Pesce, A. Treves, *The environment of the BL Lacertae object PKS 2155-304*, *Astrophys. J.* **411** (1993) L63.
- [68] A. Abramowski *et al.* [H.E.S.S. Collaboration], *H.E.S.S. and Fermi-LAT discovery of gamma rays from the blazar 1ES 1312–423*, *Mon. Not. Roy. Astron. Soc.* **434** (2013) 1889 [arXiv:1306.3186 [astro-ph.HE]].
- [69] T. A. Rector *et al.*, *The properties of the X-ray-selected EMSS sample of BL Lac objects*, *Astron. J.* **120** (2000) 1626 [astro-ph/0006215].
- [70] V. A. Acciari *et al.* [VERITAS Collaboration], *VERITAS Discovery of > 200 -GeV*

Gamma-ray Emission from the Intermediate-frequency-peaked BL Lac Object W Comae, *Astrophys. J.* **684** (2008) L73 [arXiv:0808.0889 [astro-ph]].

- [71] F. Aharonian [H.E.S.S. Collaboration], *Discovery of VHE gamma-rays from the high-frequency-peaked BL Lac object RGB J0152+017*, *Astron. Astrophys.* **481** (2008) L103 [arXiv:0802.4021 [astro-ph]].
- [72] S. A. Laurent-Muehleisen *et al.*, *Radio-loud active galaxies in the northern ROSAT all-sky survey. 3. New spectroscopic identifications from the RGB BL Lac survey*, *Astrophys. J. Suppl.* **118** (1998) 127 [astro-ph/9711268].
- [73] F. Acero [H.E.S.S. Collaboration], *PKS 2005-489 at VHE: Four Years of Monitoring with HESS and Simultaneous Multi-wavelength Observations*, *Astron. Astrophys.* **511** (2010) A52 [arXiv:0911.2709 [astro-ph.CO]].
- [74] R. Falomo *et al.*, *The redshift of the BL Lacertae object PKS 2005-489*, *Astrophys. J.* **318** (1987) L39.
- [75] F. Aharonian *et al.* [H.E.S.S. Collaboration], *Discovery of VHE gamma-rays from the BL Lac object PKS 0548-322*, *Astron. Astrophys.* **521** (2010) A69 [arXiv:1006.5289 [astro-ph.HE]].
- [76] B. Sbarufatti *et al.*, *Optical spectroscopy of BL Lacertae objects. Broad lines, companion galaxies and redshift lower limits*, *Astron. Astrophys.* **457** (2006) 35 [astro-ph/0605448].
- [77] V. Fallah Ramazani *et al.* [MAGIC Collaboration], *All the MAGIC of extreme blazars, Extreme19* (2019), available at: https://agenda.infn.it/event/15975/contributions/32047/attachments/60116/71033/EHBL_extreme19_V1.pdf
- [78] J. Becerra Gonzalez *et al.*, *Redshift determination of the very high energy gamma-ray extreme blazar PGC 2402248*, *Astron. Telegram* 11621 (2018).
- [79] F. Aharonian *et al.*, *Detection of TeV gamma-rays from the BL Lac 1ES 1959+650 in its low states and during a major outburst in 2002*, *Astron. Astrophys.* **406** (2003) L9.
- [80] S. van Velzen, H. Falcke, P. Schellart, N. Nierstenhoefer and K. H. Kampert, *Radio galaxies of the local universe: all-sky catalog, luminosity functions, and clustering*, *Astron. Astrophys.* **544** (2012) A18 [arXiv:1206.0031 [astro-ph.CO]].
- [81] G. Colonna *et al.* [H.E.S.S. Collaboration], *Spectral characteristics of Mrk 501 during the 2012 and 2014 flaring states*, *PoS ICRC 2015* (2016) 761 [arXiv:1509.04458 [astro-ph.HE]].
- [82] M. Stickel, J. W. Fried, H. Kuehr, *The complete sample of 1 Jy BL Lac objects. II - Observational data*, *Astron. Astrophys. Suppl. Ser.* **98** (1993) 393.
- [83] F. Aharonian *et al.* [HEGRA Collaboration], *Variations of the TeV energy spectrum at different flux levels of Mkn 421 observed with the HEGRA system of Cherenkov telescopes*, *Astron. Astrophys.* **393** (2002) 89 [astro-ph/0205499].
- [84] J. P. Huchra, M. J. Geller, H. G. Corwin, Jr., *The CfA Redshift Survey: Data for the NGP +36 Zone*, *Astrophys. J. Suppl.* **99** (1995) 391.

- [85] W.H. Press, B.P. Flannery, S.A. Teukolsky, W.T. Vetterling, *Numerical recipes in C : the art of scientific computing*, Cambridge : Cambridge Univ. Press, 1992.
- [86] K. Kohri and H. Kodama, *Axion-Like Particles and Recent Observations of the Cosmic Infrared Background Radiation*, *Phys. Rev. D* **96** (2017) 051701 [arXiv:1704.05189 [hep-ph]].
- [87] G. Fossati, L. Maraschi, A. Celotti, A. Comastri and G. Ghisellini, *A Unifying view of the spectral energy distributions of blazars*, *Mon. Not. Roy. Astron. Soc.* **299** (1998) 433 [astro-ph/9804103].
- [88] E. T. Meyer, G. Fossati, M. Georganopoulos and M. L. Lister, *From the Blazar Sequence to the Blazar Envelope: Revisiting the Relativistic Jet Dichotomy in Radio-loud AGN*, *Astrophys. J.* **740** (2011) 98 [arXiv:1107.5105 [astro-ph.CO]].
- [89] G. Ghisellini and F. Tavecchio, *Fermi/LAT broad emission line blazars*, *Mon. Not. Roy. Astron. Soc.* **448** (2015) 1060 [arXiv:1501.03504 [astro-ph.HE]].
- [90] M. L. Ahnen *et al.* [MAGIC Collaboration], *Detection of very high energy gamma-ray emission from the gravitationally-lensed blazar QSO B0218+357 with the MAGIC telescopes*, *Astron. Astrophys.* **595** (2016) A98 [arXiv:1609.01095 [astro-ph.HE]].
- [91] L. Foffano *et al.*, *A new hard X-ray selected sample of extreme high-energy peaked BL Lac objects and their TeV gamma-ray properties*, *Mon. Not. Roy. Astron. Soc.* **486** (2019) 1741, [arXiv:1903.07972 [astro-ph.HE]].
- [92] J. Albert *et al.* [MAGIC Collaboration], *Unfolding of differential energy spectra in the MAGIC experiment*, *Nucl. Instrum. Meth. A* **583** (2007) 494 [arXiv:0707.2453 [astro-ph]].
- [93] G. Galanti, M. Roncadelli, A. De Angelis and G. F. Bignami, *Advantages of axion-like particles for the description of very-high-energy blazar spectra*, arXiv:1503.04436 [astro-ph.HE].
- [94] F. W. Stecker, M. A. Malkan and S. T. Scully, *Intergalactic photon spectra from the far IR to the UV Lyman limit for $0 < z < 6$ and the optical depth of the universe to high energy gamma-rays*, *Astrophys. J.* **648** (2006) 774 [astro-ph/0510449]. Erratum: *Astrophys. J.* **658** (2007) 1392.
- [95] F. W. Stecker and S. T. Scully, *Derivation of a Relation for the Steepening of TeV Selected Blazar Gamma-ray Spectra with Energy and Redshift*, *Astrophys. J.* **709** (2010) L124 [arXiv:0911.3659 [astro-ph.CO]].
- [96] D. A. Sanchez, S. Fegan and B. Giebels, *Evidence for a cosmological effect in γ -ray spectra of BL Lacs*, *Astron. Astrophys.* **554** (2013) A75 [arXiv:1303.5923 [astro-ph.HE]].
- [97] W. Essey and A. Kusenko, *On weak redshift dependence of gamma-ray spectra of distant blazars*, *Astrophys. J.* **751** (2012) L11 [arXiv:1111.0815 [astro-ph.HE]].
- [98] A. Dominguez and M. Ajello, *Spectral analysis of Fermi-LAT blazars above 50 GeV*, *Astrophys. J.* **813** (2015) no.2, L34 [arXiv:1510.07913 [astro-ph.HE]].
- [99] S. V. Troitsky, *Axion-like particles and the propagation of gamma rays over astronomical distances*, *JETP Lett.* **105** (2017) 55 [arXiv:1612.01864 [astro-ph.HE]].

- [100] T. A. Dzhatdoev, E. V. Khalikov, A. P. Kircheva and A. A. Lyukshin, *Electromagnetic cascade masquerade: a way to mimic γ -axion-like particle mixing effects in blazar spectra*, *Astron. Astrophys.* **603** (2017) A59 [arXiv:1609.01013 [astro-ph.HE]].
- [101] W. Essey and A. Kusenko, *A new interpretation of the gamma-ray observations of active galactic nuclei*, *Astropart. Phys.* **33** (2010) 81 [arXiv:0905.1162 [astro-ph.HE]].
- [102] W. Essey, O. E. Kalashev, A. Kusenko and J. F. Beacom, *Secondary photons and neutrinos from cosmic rays produced by distant blazars*, *Phys. Rev. Lett.* **104** (2010) 141102 [arXiv:0912.3976 [astro-ph.HE]].
- [103] G. Rubtsov, P. Satunin and S. Sibiryakov, *Prospective constraints on Lorentz violation from ultrahigh-energy photon detection*, *Phys. Rev. D* **89** (2014) 123011 [arXiv:1312.4368 [astro-ph.HE]].
- [104] G. Rubtsov, P. Satunin and S. Sibiryakov, *Constraints on violation of Lorentz invariance from atmospheric showers initiated by multi-TeV photons*, *JCAP* **1705** (2017) 049 [arXiv:1611.10125 [astro-ph.HE]].
- [105] H. Abdalla and M. Bottcher, *Lorentz Invariance Violation Effects on Gamma-Gamma Absorption and Compton Scattering*, *Astrophys. J.* **865** (2018) 159 [arXiv:1809.00477 [astro-ph.HE]].
- [106] G. Raffelt and L. Stodolsky, *Mixing of the Photon with Low Mass Particles*, *Phys. Rev. D* **37**, 1237 (1988).
- [107] C. Csaki, N. Kaloper, M. Peloso and J. Terning, *Super GZK photons from photon axion mixing*, *JCAP* **0305** (2003) 005 [hep-ph/0302030].
- [108] A. De Angelis, M. Roncadelli and O. Mansutti, *Evidence for a new light spin-zero boson from cosmological gamma-ray propagation?*, *Phys. Rev. D* **76** (2007) 121301 [arXiv:0707.4312 [astro-ph]].
- [109] M. Simet, D. Hooper and P. D. Serpico, *The Milky Way as a Kiloparsec-Scale Axionscope*, *Phys. Rev. D* **77** (2008) 063001 [arXiv:0712.2825 [astro-ph]].
- [110] M. Fairbairn, T. Rashba and S. V. Troitsky, *Photon-axion mixing and ultra-high-energy cosmic rays from BL Lac type objects - Shining light through the Universe*, *Phys. Rev. D* **84** (2011) 125019 [arXiv:0901.4085 [astro-ph.HE]].
- [111] S. Troitsky, *Towards discrimination between galactic and intergalactic axion-photon mixing*, *Phys. Rev. D* **93** (2016) 045014 [arXiv:1507.08640 [astro-ph.HE]].
- [112] S. Abdollahi *et al.* [Fermi-LAT Collaboration], *A gamma-ray determination of the Universe's star formation history*, *Science* **362** (2018) 1031 [arXiv:1812.01031 [astro-ph.HE]].

Table 1. List of blazars selected for the main sample as described in the text. Classes: B=BLL, F=FSRQ. Instruments: H=HESS, L=Fermi LAT, M=MAGIC, V=VERITAS. Note: the symbol in the last column means the source does not satisfy the (S2) criterion for both the Franceschini et al. (2017) and Gilmore et al. 2012 fixed (*) or for Korochkin and Rubtsov 2018 (†) EBL models, respectively.

Name	Redshift	Class	Instrument	Ref. (spec.)	Ref. (z)	Note
B2 2114+33	1.596	F	L		[30]	*
GB6 J0043+3426	0.966	F	L		[31]	
PKS 1441+25	0.939	F	M	[32]	[31]	
4C +55.17	0.896	F	L		[33]	*
PKS 0537−441	0.892	F	L		[34]	*
PG 1246+586	0.847	B	L		[35]	
Ton 0599	0.725	F	M	[36]	[37]	
PKS 1424+240	0.605	B	V	[38]	[39]	
3C 279	0.536	F	M	[40]	[41]	
4C +21.35	0.432	F	M	[42]	[43]	
PKS 1510−089	0.360	F	M	[44]	[45]	
OT 081	0.322	B	H	[46]	[47]	
OJ 287	0.306	F	V	[48]	[49]	
1ES 0414+009	0.287	B	H	[50]	[51]	
1RXS J023832.6−311658	0.233	B	H	[52]	[30]	
1ES 1011+496	0.212	B	M	[53]	[54]	
1ES 1218+304	0.182	B	V	[55]	[56]	
H 2356-309	0.165	B	H	[57]	[58]	
1ES 0229+200	0.140	B	V	[59]	[60]	
1ES 0806+524	0.138	B	M	[61]	[62]	
1ES 1215+303	0.131	B	M	[63]	[39]	
H 1426+428	0.129	B	HEGRA	[64]	[65]	
PKS 2155−304	0.116	B	H	[66]	[67]	
1ES 1312−423	0.105	B	H	[68]	[69]	†
W Com	0.102	B	V	[70]	[39]	*
RGB J0152+017	0.080	B	H	[71]	[72]	
PKS 2005−489	0.071	B	H	[73]	[74]	
PKS 0548−322	0.069	B	H	[75]	[76]	*
PGC 2402248	0.065	B	M	[77]	[78]	*
1ES 1959+650	0.048	B	HEGRA	[79]	[80]	
Mrk 501	0.034	B	H	[81]	[82]	
Mrk 421	0.031	B	HEGRA	[83]	[84]	

Table 2. Results of the analysis performed with various models of pair-production opacity discussed in the text. Number of objects in the sample and the significance of breaks at $E_0(z)$ are given.

EBL model	Number of objects	Significance, σ
Korochkin and Rubtsov (2018)	31	1.9
Gilmore et al. (2012) fixed	26	1.3
Franceschini et al. (2017)	26	1.5
Upper-limit EBL normalized to [6, 14]	29	>10

Table 3. Significance of the distance-dependent spectral hardenings for subsamples including objects observed by different instruments.

Instruments	Number of objects	Significance
MAGIC + HESS + VERITAS	23	1.9σ
MAGIC + HESS + LAT	23	2.4σ
MAGIC + VERITAS + LAT	19	1.7σ
HESS + VERITAS + LAT	19	1.7σ

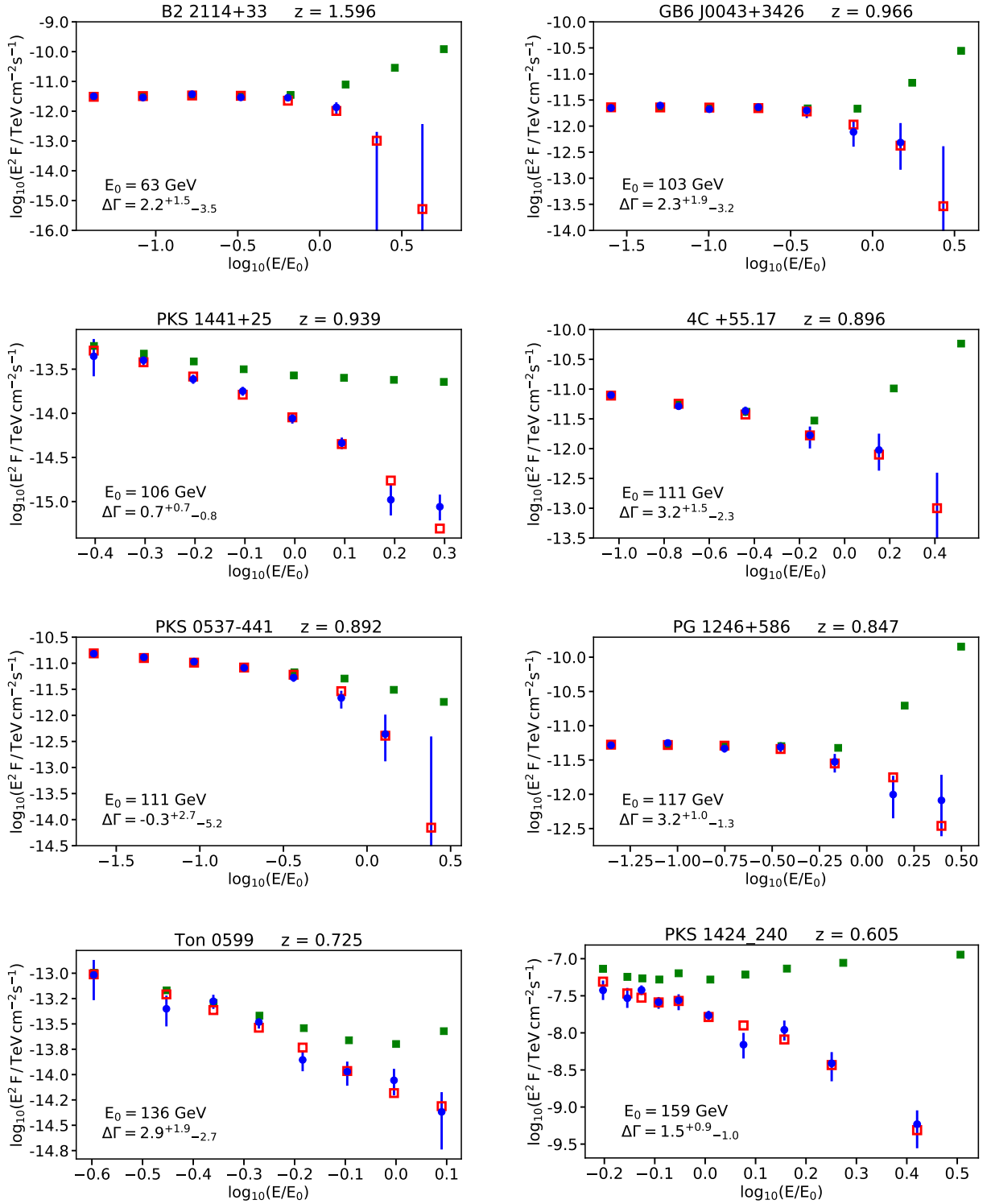


Figure 13. Spectra of 31 blazars from the sample studied in this work (bin-by-bin fluxes). Blue circles with error bars: observed spectra; green boxes: best fit of the intrinsic spectrum with the break at the energy E_0 for which $\tau(E_0, z) = 1$. Red open boxes indicate bin-by-bin fluxes corresponding to the best-fit spectra after absorption. Names of the sources, values of their redshifts z , energies E_0 and break strengths $\Delta\Gamma$ are shown on the plots. See the main text for more details.

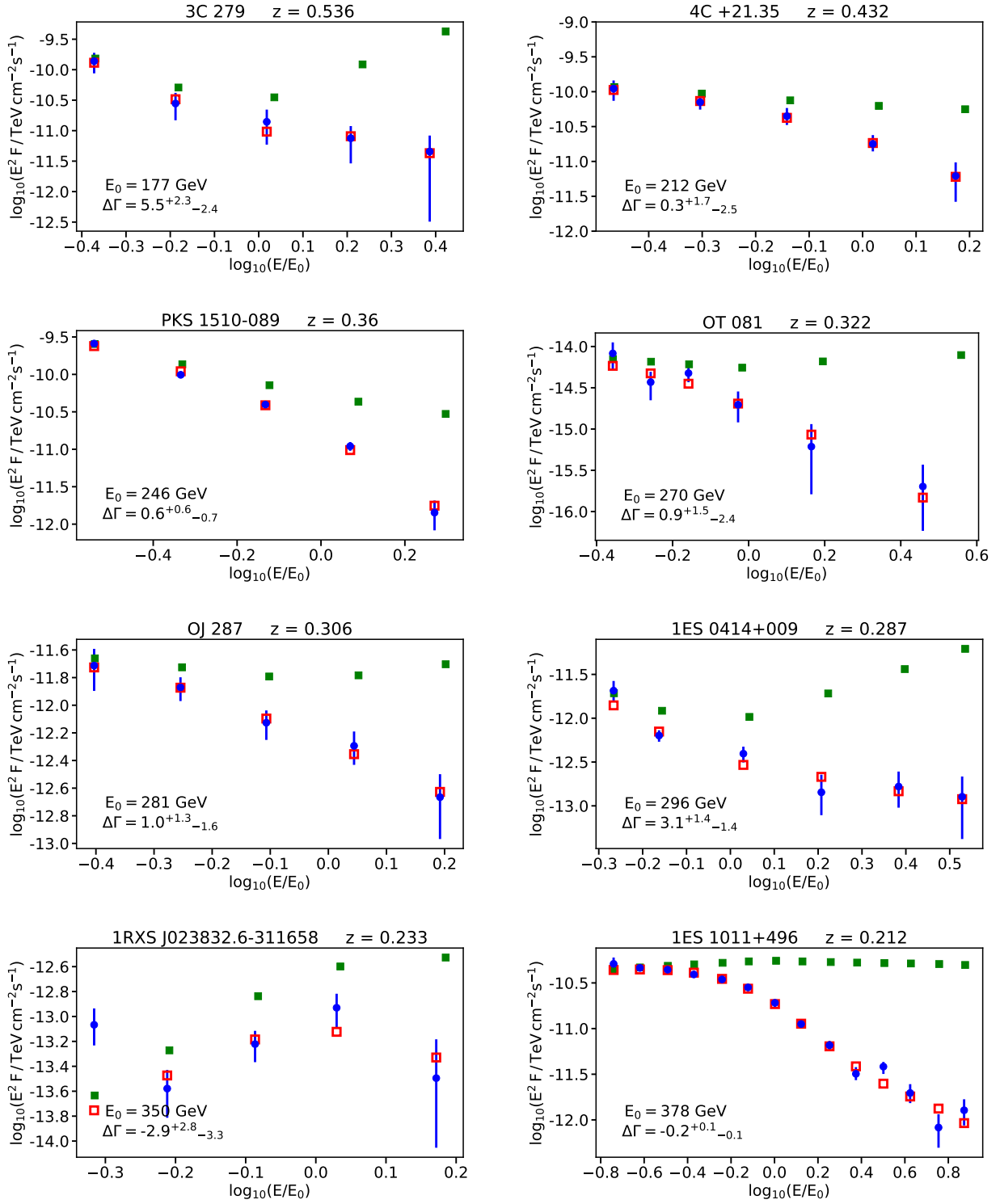


Figure 14. Continuation of Fig. 13.

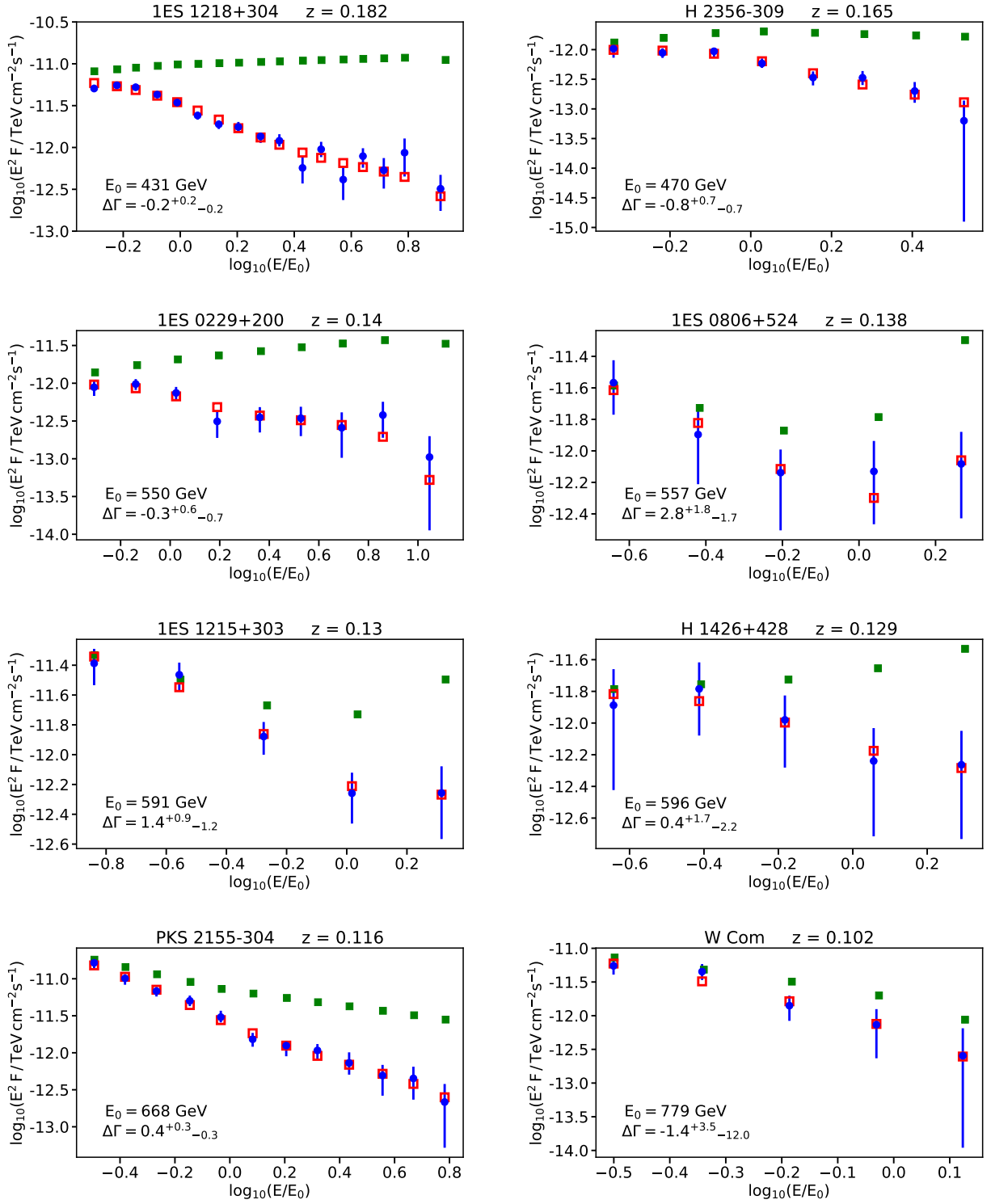


Figure 15. Continuation of Fig. 13.

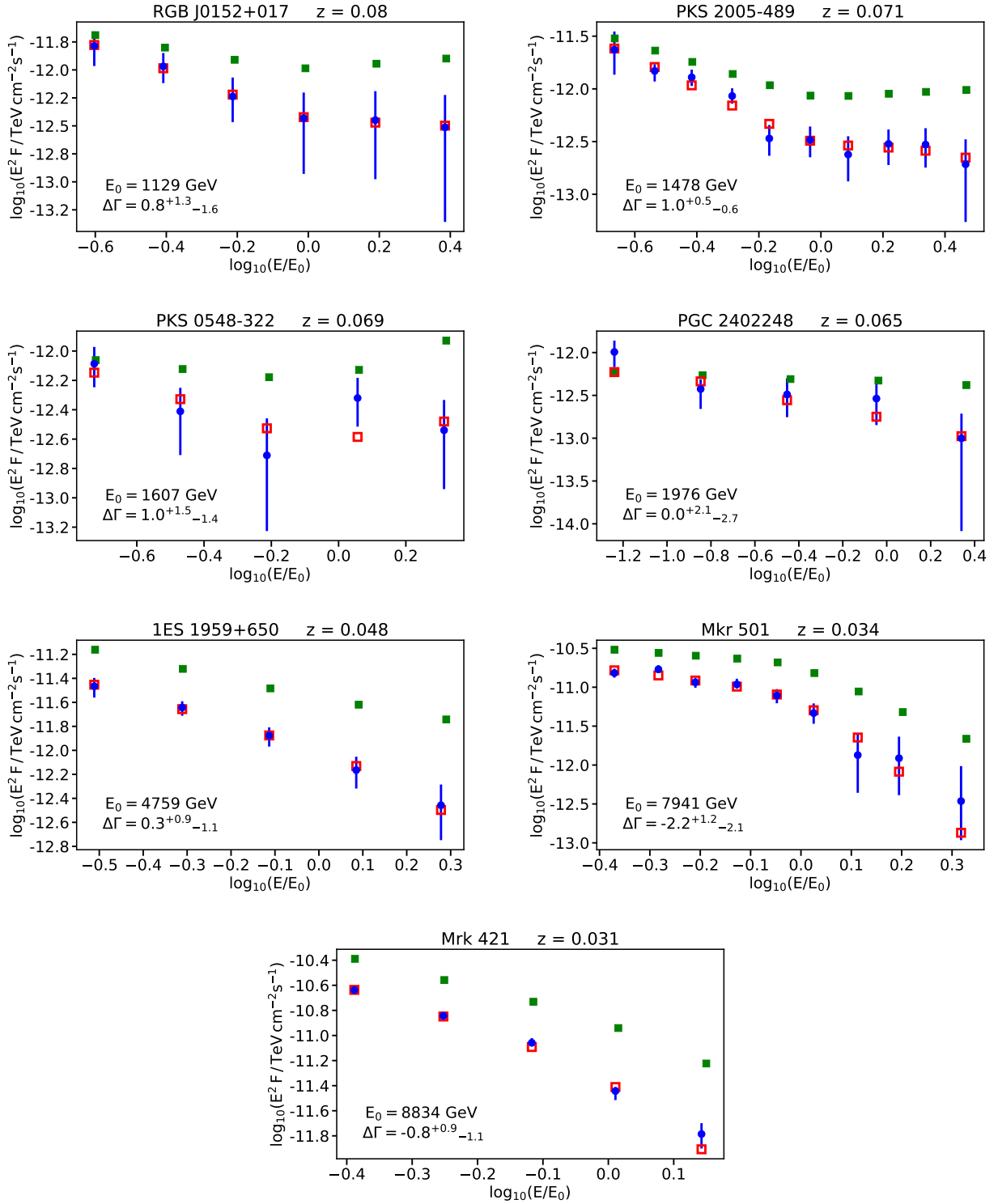


Figure 16. Continuation of Fig. 13.